3D PRINTED-POLY(LACTIC ACID) SCAFFOLDS WITH IMPROVED BIOACTIVITY FOR BONE TISSUE ENGINEERING

Bruna Nunes Teixeira

Tese de Doutorado apresentada ao Programa de Pós-graduação em Engenharia Metalúrgica e de Materiais, COPPE, da Universidade Federal do Rio de Janeiro, como parte dos requisitos necessários à obtenção do título de Doutor em Engenharia Metalúrgica e de Materiais.

Orientador: Rossana Mara da Silva Moreira Thiré

Rio de Janeiro

Dezembro de 2017

3D PRINTED- POLY(LACTIC ACID) SCAFFOLDS WITH IMPROVED BIOACTIVITY FOR BONE TISSUE ENGINEERING

Bruna Nunes Teixeira

TESE SUBMETIDA AO CORPO DOCENTE DO INSTITUTO ALBERTO LUIZ COIMBRA DE PÓS-GRADUAÇÃO E PESQUISA DE ENGENHARIA (COPPE) DA UNIVERSIDADE FEDERAL DO RIO DE JANEIRO COMO PARTE DOS REQUISITOS NECESSÁRIOS PARA A OBTENÇÃO DO GRAU DE DOUTOR EM CIÊNCIAS EM ENGENHARIA METALÚRGICA E DE MATERIAIS.

Examinada por:

_____

Prof. Rossana Mara da Silva Moreira Thiré, D.Sc.

_____

Prof. José Antônio da Cunha Ponciano Gomes, D.Sc.

_____

Prof. Daniel John Kelly, PhD.

_____

Prof. Renata Nunes Oliveira, D.Sc.

_____

Prof. Gutemberg Gomes Alves, D.Sc.

RIO DE JANEIRO, RJ – BRASIL

DEZEMBRO DE 2017

Teixeira, Bruna Nunes

3D printed-poly(lactic acid) scaffolds with improved bioactivity for bone tissue engineering/ Bruna Nunes Teixeira – Rio de Janeiro: UFRJ/COPPE, 2017

X, 85 p.: il.; 29.7 cm.

Orientador: Rossana Mara da Silva Moreira Thiré.

Tese (Doutorado) – UFRJ/ COPPE/ Programa de Engenharia Metalúrgica e de Materiais, 2017.

Referências Bibliográficas: p. 75-83.

1. Surface modification. 2. Poly(lactic acid). 3. Scaffolds. 4. 3D Printing. 5. Bone Tissue Engineering. I. Thiré, Rossana Mara da Silva Moreira II. Universidade Federal do Rio de Janeiro, COPPE, Programa de Engenharia Metalúrgica e de Materiais. III. Título

To my mother, Marlice N. Teixeira, my treasure. Thank you for teaching me, among other things, how important is to study. This is our victory!!!

Acknowledgments

First of all, I thank God for making this achievement possible, blessing and protecting me all the time.

To my Brazilian advisor, Dr Rossana Thiré. Thank you so much for trusting me and seeing virtues that even I couldn't. Thank you for accepting me as a member of the group, back in 2010, and for continuing with me, believing it would be possible! Thank you for being by my side and motivating me!

To my Irish advisor and PI, Prof. Danny Kelly. Thank you for your support, patience and supervision during the year that I was in Dublin. To be a temporary member of your research group made me grow up as a professional and as a person. I learned so many things! Thanks a million!!!!

No victory happens by individual effort. My parents, my safe harbor, who have never leave me helpless. Not even all the thanks in the world would be enough to phrase how essential you have been in my life. I love you from the bottom of my heart! To my sister, best friend and biggest fan Kelly, that is always filling me up with her love. This is our moment!!!! To my nephew and niece, Gustavo and Giulia, thanks for always cheering for me.

Thanks to my uncles and aunts, godfather, cousins and other relatives. Thanks for being so caring and so concerned about me. You are part of this!

To my friends, who kindly gave me to my Doctorate. Especially my dearest and special friends, Aline and Camylle, who always held my hand and had all the patience of the world with me! My dear friend Renatinha (neeeeem), that is my shoulder to cry in so many moments. Roberta, Taila, Silvia and Marcio, friends that the little Biopoli gave me! To the friends that Ireland gave me, especially my sister Gracieli and my beloved Fernando and Erik. You made me feel loved and special!

To my lab friends and colleagues, PH, Dahyna, Tais, Flávia, Aline, Jean, Javier, Marceli e João. Thank you guys! All of you made my days lighter and much happier. And, how can I forget the best gift that COPPE gave me? It is impossible not to thank all the partnership and friendship that both of you, Caroline and Marianna, gave me. I will keep you two in my heart forever!! I love you girls.

Many thanks to my friends and colleagues from TCBE. Guys, all of you are awesome! Thanks to be, always, so kind and patient with me. A special thanks to Dinorath, Paola, Swetha and Grainné.

To all PEMM professors and employees. Thank you so much for being so special and always so professional.

To CNPq and FAPERJ for financial support

Resumo da Tese apresentada à COPPE/UFRJ como parte dos requisitos necessários para a obtenção do grau de Doutor em Ciências (D.Sc.)

ARCABOUÇOS DE POLI(LÁCTICO ÁCIDO) PRODUZIDOS POR IMPRESSÃO 3D COM BIOATIVIDADE MELHORADA PARA ENGENHARIA DE TECIDO ÓSSEO

Bruna Nunes Teixeira

Dezembro/2017

Orientador: Rossana Mara da Silva Moreira Thiré

Programa: Engenharia Metalúrgica e de Materiais

Arcabouços de poli(ácido láctico) (PLA) produzidos por impressão 3D são uma alternativa promissora na engenharia tecidual. A funcionalização da superfície baseada no modelo de mexilhão – Polidopamina (PDA), foi proposta como uma maneira eficiente de aumentar a bioatividade e promover a imobilização covalente de biomoléculas, tais como o colágeno (COL) tipo I, nas superfícies. Este estudo teve como objetivo caracterizar arcabouços de PLA produzidos por impressão 3D, com diferentes espaçamentos entre os filamentos, concomitantemente à influência do recobrimento com PDA como plataforma para aumentar a bioatividade e a imobilização de COL I na superfície dos arcabouços. A geometria influenciou diretamente na porosidade e na resistência à compressão das peças impressas. A camada de PDA melhorou a imobilização de COL I na superfície dos arcabouços em 92% e aumentou a adesão de células-tronco mesenquimais. A sobreposição de PDA e COL I forneceu as melhores condições para adesão celular e proliferação no estágio inicial da cultura celular. Além disso, nessa condição, células produziram quantidade expressivamente maior de fosfatase alcalina, um conhecido marcador de osteogênese, após 21 dias em cultura. Os arcabouços com poros projetados de 700 μm (espaçamento intermediário = 1 mm) e revestidos com PDA/COL proporcionam porosidade, tamanho de poro, propriedades mecânicas e condições biológicas adequadas para permitir a regeneração do tecido ósseo.

Abstract of Thesis presented to COPPE/UFRJ as a partial fulfillment of the requirements for the degree of Doctor of Science (D. Sc.)

3D PRINTED-POLY(LACTIC ACID) SCAFFOLDS WITH IMPROVED BIOACTIVITY FOR BONE TISSUE ENGINEERING

Bruna Nunes Teixeira

December/2017

Advisor: Rossana Mara da Silva Moreira Thiré

Department: Metallurgical and Materials Engineering

PLA scaffolds produced by 3D printing are a promising alternative to bone tissue engineering. A simple mussel inspired method, polydopamine (PDA) surface functionalization, has being proposed as an efficient way to enhance the bioactivity of biomaterials, such as PLA, and to promote covalent immobilization of a variety of proteins such as collagen (COL) type I. This study aimed to characterize PLA scaffolds produced by FDM with different pore size, concomitantly to the influence of PDA coating as platform to enhance the bioactivity and the immobilization of COL I onto printed PLA. Scaffolds geometry influenced directly in the porosity and compressive strength of printed parts. The PDA layer improved the COL immobilization onto the surface of PLA scaffolds in 92% and enhanced the adhesion of porcine Bone Marrow Stem Cells (MSCs). The combination of PDA and COL layers provided the best conditions for early stage cell adhesion and proliferation. Cells cultured onto PDA/COL scaffolds produced substantially higher amounts of Alkaline Phosphatase (ALP), a marker of osteogenesis, by 21 days in culture. Scaffolds with projected pores of 700 μm in size (strut spacing = 1 mm) and coated with PDA plus COL I provides appropriate porosity, mechanical properties and biological conditions to allow bone tissue regeneration.

Contents

1. Introduction

Tissue engineering (TE) involves the application of principles and methods of engineering and biomedical sciences to develop biological substitutes to restore, to maintain or to improve functions of damaged tissues (NEREM; SAMBANIS, 1995; O'BRIEN, 2011; VACANTI; LANGER, 1999). Bone tissue is able to self-healing, however in cases of critically sized bone defects resulting from trauma or congenital diseases, the tissue cannot self-regenerate, necessitating further intervention to guide the healing (FERNANDEZ-YAGUE et al., 2015; KANCZLER, 2008). In these cases, TE has been widely applied to found an efficient way to restore the damaged site (ATALA, 2007; OKANO, 2014; SHAFIEE; ATALA, 2017; STEVENS, 2008; SUSMITA BOSE; BANDYOPADHYAY, 2012). TE encompasses different approaches and one of them comprises the use of solid and porous matrices (scaffolds), which can be loaded with specific growth factors and cell lines to *in vitro* culture (ATALA, 2007; TROHATOU; ROUBELAKIS, 2017). Scaffolds guide the development of a new tissue, providing mechanical stability and a three-dimensional environment for cells, which allows them to adhere, proliferate, differentiate and secrete extracellular matrix (ECM), leading to tissue reconstruction (ATALA, 2012; NADERI; MATIN; BAHRAMI, 2011).

Scaffold geometry plays a key role in define neo-tissue formation (JAFARI et al., 2015; SOUNESS et al., 2017). While porosity is fundamental to nutrient and oxygen transport to cells that are cultivated inside a scaffold, pore size will directly affect tissue deposition and differentiation. The ideal pore size for osteogenesis *in vitro* is believed to be in the range of 100 and 250 μm, although pores in the range of 300-800 μm might better support both bone formation and vascularisation (MURPHY; HAUGH;

O'BRIEN, 2010; SUSMITA BOSE; BANDYOPADHYAY, 2012). However, increasing scaffold porosity/pore size can result in scaffolds with poor mechanical properties. Therefore, the balance between scaffold porosity/pore size and biological and mechanical properties is necessary to create an efficient matrix to lead bone tissue regeneration.

Conventional methods to manufacture polymeric scaffolds have some limitations that restrict their applications. Among these limitations, the manual intervention, the poor reproducibility, the use of toxic organic solvents and the difficulty to produce scaffolds with controlled geometry can be highlighted (HUTMACHER et al., 2007; SEARS et al., 2016). Additive manufacturing technologies (AM), commonly called 3D-printing technologies, have been used as an alternative to overcome these problems. AM technologies allow to produce devices with high complexity in macro and micro structures from 3D model data, in a layer-by-layer process (KIM; SHIN; LIM, 2012; O'BRIEN et al., 2015; VAEZI; SEITZ; YANG, 2013).

Fused deposition modeling (FDM) is an AM technique in which a thermoplastic filament is melted in a heated-head connected to a carriage moving in the horizontal xy plane. The head-heated deposits the material through a nozzle directly on to the build platform, following a programmed path. When a layer is deposited, the platform moves down in the z direction to deposit the next layer (BOSCHETTO; BOTTINI, 2014; MOHAMED; MASOOD; BHOWMIK, 2015; ZIEMIAN; CRAWN, 2001). The selection of raw material is one of the keys for 3D scaffolds fabrication, since it will affect the final properties of the biomaterial, such as mechanical properties, biodegradability and biocompatibility (HUTMACHER et al., 2007; SUSMITA BOSE; BANDYOPADHYAY, 2012). In this context, poly(lactic acid) (PLA) has attracted

attention of scientific community due to its biocompatibility, biodegradability, ease of processing and thermal stability (RASAL; HIRT, 2010; SANTORO et al., 2016). The main product of PLA degradation, in mammal's body, is the α-hydroxy acid, which is incorporated by the carboxylic acid cycle and completely excreted. PLA is approved by Food and Drug Administration (FDA) to applications that require direct contact with biological fluids (CARRASCO et al., 2010; RASAL; HIRT, 2010). However, PLA is a hydrophobic polymer with low bioactivity, thus it is necessary to improve its surface properties to allow cell interactions (SERRA et al., 2013).

Collagen, as the major organic component of bone extracellular matrix, is frequently used to improve cellular activity, such as adhesion, proliferation and differentiation onto biomaterial surfaces. Although numerous strategies have been developed to immobilize collagen onto a PLA scaffold surface, most of these methods involve complicated chemistry which usually introduces extra toxic factors (CHENG; TEOH, 2004; SOUSA et al., 2014; WANG et al., 2015b). Inspired in the way that mussels strongly adhere to a variety of surfaces, a simple and one step mussel-inpired polydopamine (PDA) method has been proposed by Messersmith's group to improve the bioactivity of biomaterials surface and the immobilization of proteins and other biomolecules, as COL (KAO et al., 2015; LEE et al., 2007).

In this study, PLA scaffolds with different pore size were manufactured via FDM. Constructs were coated with PDA and COL, in order to enhance their bioactivity. The effect of different pore size on to the physical properties of PLA scaffolds was evaluated by dimensional deviation of printed parts in comparison with designed model, Archimedes Principle to estimate porosity and mechanical properties under compressive load. To evaluate the efficiency of PDA and COL immobilization, scaffolds were analysed by X-ray photoelectron spectroscopy (XPS), atomic force microscopy (AFM)

and biochemical assay to measure COL content. The biological response to PLA scaffolds with different pore size and different coatings was evaluated by in *vitro culture* of porcine Bone Marrow Stem Cells (MSCs) for 21 days. Cell viability, adhesion, morphology, metabolic activity and production of osteogenic marker were analysed.

2. Literature Review

2.1. Tissue Engineering

Extended in life expectation and the recent advances in biomedical sciences justifies the search for effective alternatives to restore damages in tissue and organs (CHEN; LIU, 2016; NEREM; SAMBANIS, 1995). The limitations in the techniques that are currently applied to restore tissues and organs are challenges to doctors and researchers overcome. As example, the shortage of donors in opposite to large amount of patients requiring organs transplants is a key point that supports the research for new alternatives in regenerative medicine.

Tissue engineering (TE) is a regenerative medicine tool, which involves the application of principles and methods of engineering and biomedical sciences to develop biological substitutes to restore, to maintain or to improve functions of damaged tissues (NEREM; SAMBANIS, 1995; O'BRIEN, 2011; VACANTI; LANGER, 1999). The different approaches of TE includes (ATALA, 2007):

1. Acellular matrix (artificial scaffolds or part of live tissues undergone to decellularization process) which stimulate the body abilities to guide and orientate the new tissue growth;
2. Matrix with embedded cells (when implanted, these matrix are degraded slowly, being substituted by the extracellular matrix produced by cells);
3. Delivery of signalization molecules for growth and/or differentiation, important for cell recognizing and tissue regeneration;

4. Delivery of cells in solution or cells embedded in hydrogels, which are inserted directly on the damage tissue. These cells are stimulated by proliferation signalling molecules, contributing for tissue regeneration.

To realize the mechanism related to the well-working of a live tissue is fundamental to produce a biological substitute that can play, efficiently, specific functions of a target tissue/organ. Different types of cells can be applied for tissue regeneration. Amongst them, embryonic stem cells, adult stem cells, linage of progenitor cells specific for each tissue and pluripotent stem cells with induced differentiation (TROHATOU; ROUBELAKIS, 2017).

Bone is a highly vascularised tissue that has the potential to spontaneously regenerate, however, in cases of critically sized defect from traumas or congenital diseases, this self-regeneration cannot occur, when it is necessary some intervention to guide the regeneration (FERNANDEZ-YAGUE et al., 2015; KANCZLER, 2008). In these cases, TE has been widely applied to find an efficient way to restore the damaged site (ATALA, 2007; OKANO, 2014; SHAFIEE; ATALA, 2017; STEVENS, 2008; SUSMITA BOSE; BANDYOPADHYAY, 2012).

2.1.2. Bone Tissue Engineering

Bone tissue engineering is a dynamic and complex process, which begins with the recruitment and migration of osteoprogenitors cells, followed by cell proliferation, differentiation, bone matrix deposition and remodelling of new tissue (SUSMITA BOSE; BANDYOPADHYAY, 2012). Bone injury is defined as a discontinuity in the

bone integrity as a result of trauma, congenital malformation or surgical intervention. When a critical defect occurs or in some medical conditions (elderly people, diabetes, osteoporosis, etc) it is necessary to do a surgical intervention to restore the tissue integrity (SHRIVATS; MCDERMOTT; HOLLINGER, 2014).

Bone is a variation of conjunctive tissue, whose function is the internal support of vertebrates and regulation of Calcium (Ca^{+}) levels on the blood. Their cells secrete proteins and polysaccharides, that are deposited in an organized way, forming the ECM (WANG et al., 2015a). Bone ECM is mineralized, reinforced by calcium salt and composed, mostly, by collagen type I. Other bone ECM compounds are proteoglycans and non-collagen proteins. There are two forms of bone tissue: the cortical bone (which is responsible for mechanical properties and to protect the whole bone tissue) and the cancellous bone (metabolic functions) (Figure 2.1) (HUTMACHER et al., 2007). Four cell types are, mainly, founded in this tissue (FLORENCIO-SILVA et al., 2015):

1. Osteoblasts – Founded in bone surface, are responsible to secrete the BCM. When they are in intense synthetic activity, they have a cuboid shape;
2. Osteoclasts – Founded in bone surface, responsible for BCM resorption, They act in bone renewing;
3. Mesenchymal cells – Precursors of osteoblasts;
4. Osteocytes – Mature osteoblasts soaked in mineralized BCM, are responsible for matrix maintenance.

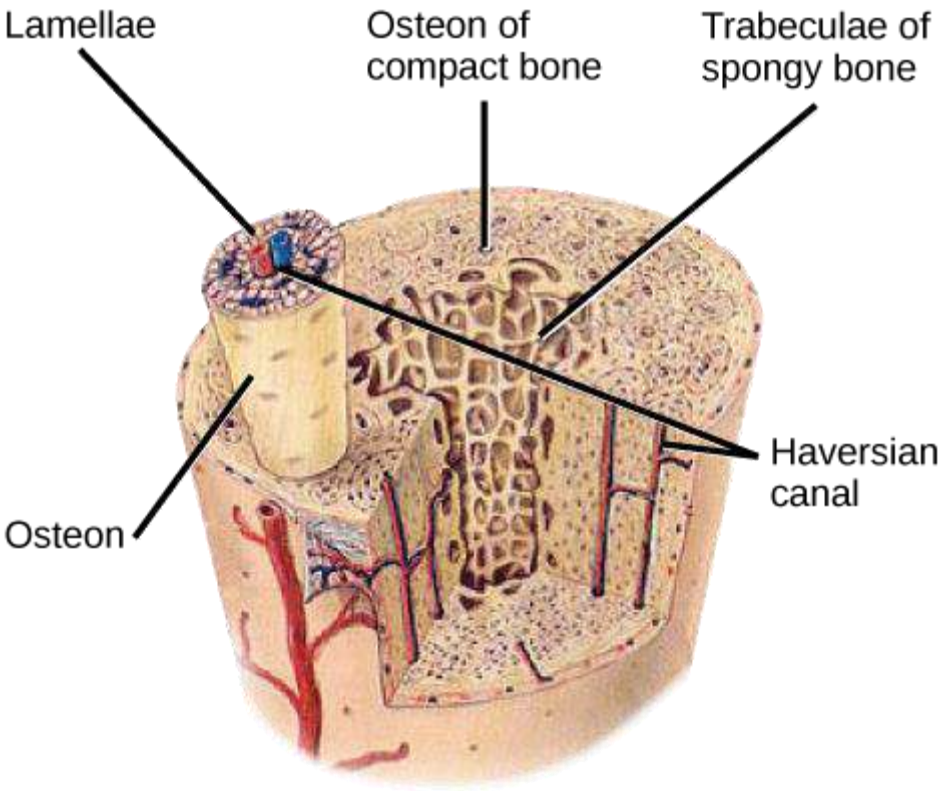

Fig. 2.1. Bone basic structure (https://s3-us-west-2.amazonaws.com/courses-images/wp-content/uploads/sites/1223/2017/02/08000637/Figure_38_02_04.png)

Bone is divided, basically, in two different morphologies: trabecular or cancellous bone, with 50–90% porosity and pore sizes at the order of 1mm in diameter; the cortical bone is surrounding it and it has a solid structure with voids, such as haversian canals, with a cross-sectional area of 2500–12,000 mm^2, with 3–12% porosity. The degree of mineralization for bone tissue varies according to the functionality. Mechanical properties of bone tissue is dependent on age and it is reported that, after bone maturation, the tensile strength and modulus of elasticity of femoral cortical bone, for example, reduces approximately 2% per decade (KARAGEORGIOU; KAPLAN, 2005).

Bone is a tissue with complex architecture and properties. Differences in porosity, pore size, mechanical properties, degree of mineralization that are dependent of age, nutritional state, activity and diseases impose a major challenge to produce successful scaffolds for bone tissue engineering that will meet the needs of specific repair sites in specific patients (KARAGEORGIOU; KAPLAN, 2005).

2.2. Scaffolds for Bone Tissue engineering

TE encompasses different approaches and one of them comprises the use of solid and porous matrices (scaffolds), which can be *in vitro* cultured with cell lines and specific growth factors (ATALA, 2007; TROHATOU; ROUBELAKIS, 2017). Scaffolds will guide the development of a new tissue, providing mechanical stability and became possible a three-dimensional organization for cells, which will allows them to adhere, proliferate, differentiate and secrete extracellular matrix (ECM), leading to tissue reconstruction (ATALA, 2012; NADERI; MATIN; BAHRAMI, 2011).

The ideal scaffold for bone tissue regeneration should mimic bone ECM characteristics and should support cell adhesion, proliferation and differentiation (WU et al., 2014). The geometry and architecture of scaffolds plays a key role in define neo-tissue formation (JAFARI et al., 2015; SOUNESS et al., 2017). Porosity is defined as percentage of void space in a solid and is fundamental to promote the flow of nutrients and oxygen to cells that are attached inside the scaffold besides to allow adequate cellular migration trough scaffolds structure. Pore size will directly affect tissue deposition and differentiation. Minimum pore sized required to regenerate mineralized bone is generally considered to be 100 μm. Nevertheless the ideal pore size for osteogenesis *in vitro* is believed to be in the range of 100 and 250 μm. However pores in

the range of 300-800 μm might better support both bone formation and vascularisation (MURPHY; HAUGH; O'BRIEN, 2010; SUSMITA BOSE; BANDYOPADHYAY, 2012).

Murphy et al. (2016) evaluated the effect of different pore sizes (85 - 325μm) on osteoblasts differentiation and ECM mineralization. They prepared collagen-glycosaminoglycan scaffolds by lyophilisation with 5 different porosities and cultivated them with either mesenchymal stem cells (MSCs) or mature osteoblasts for 42 days. A 325 μm pore size allowed for better osteoblast penetration into the bulk of the scaffold, and promoted the earlier expression of osteopontin and osteocalcin as well as an increase in the matrix mineralization. The MSCs behaviour was similar to that of the osteoblasts, although MSCs motility, proliferation and infiltration were reduced when in comparison with osteoblasts. The authors concluded that although large pores can promote a better cell interaction with collagen-glycosaminoglycan scaffolds, the ideal pore size to design an efficient construct for bone tissue engineering is dependent of the chosen cell type (MURPHY et al., 2016) .

Taniguchi et al. (2016) evaluated the effect of pore size with constant porosity on *in vivo* bone ingrowth in rabbits into porous titanium implants manufactured by Selective laser melting (SLM). Three porous titanium implants (with an intended porosity of 65% and pore sizes of 300, 600, and 900 μm, designated the P300, P600, and P900 implants, respectively) were manufactured and their porous structures were evaluated and verified by microfocus X-ray computed tomography. The average pore sizes of the P300, P600, and P900 implants were 309, 632, and 956 μm, respectively. To evaluate the implant ability to fixate on the bone, porous-surfaced titanium plates were implanted into the cortical bone of the rabbit tibia. To evaluate the potential to bone ingrowth into scaffolds structure, cylindrical porous titanium implants were placed

into the cancellous bone of the rabbit femur for 2, 4, and 8 weeks. The P600 implant demonstrated a significantly higher fixation ability at 2 weeks than the other implants. After 4 weeks, all models had sufficiently high fixation ability in a detaching test. Bone ingrowth into the P300 implant was lower than into the other implants at 4 weeks. Due to its appropriate mechanical strength, high fixation ability, and rapid bone ingrowth, the authors suggested that the pore structure of the P600 implant is a suitable porous structure for orthopedic implants manufactured by SLM (TANIGUCHI et al., 2016).

Lee et al. (2012) evaluated the effect of pore architecture and stacking direction on the mechanical properties and cell proliferation of PCL/PLGA scaffolds manufactured by solid freeform fabrication technology. Different types of scaffolds with different pore architectures (lattice, stagger, and triangle types) and stacking directions (horizontal and vertical directions) were fabricated. Triangles scaffolds had shown highest resistance under compressive load among the experimental groups. Stacking direction affected the mechanical properties of scaffolds. Pore architecture and stacking directions did not affect cell density over the culture period. The authors concluded that the mechanical properties of scaffolds can be enhanced by controlling pore architecture and stacking direction in order to adequate scaffolds for different bone sites (LEE et al., 2012).

Scaffolds with high porosity and adequate pore size tend to facilitate bone ingrowth. However, highly porous structures tends to possess poor mechanical properties, since this compromises the structural integrity of the scaffold (KARAGEORGIOU; KAPLAN, 2005). There is a limit to porosity or pore sizes into scaffolds without compromising its mechanical properties. In general, scaffolds should have sufficient mechanical strength to support cell proliferation, ECM deposition and tissue growth. Scaffolds fabricated for bone tissue engineering should have comparable

strength to the native bone tissue in order to withstand physiological loadings as well as to prevent stress shielding from occurring. Although the mechanical property of scaffolds is compromised with higher porosity or pore sizes, the use of materials with high inherent mechanical strength might be a solution to this issue (LOH; CHOONG, 2013).

2.2.1. Scaffolds production

Different methodologies are applied to manufacture scaffolds for bone tissue engineering. Conventional methods includes solvent casting and particulate leaching, gas foaming, freeze-drying etc (HUTMACHER et al., 2007). Most of them have some limitations that restrict their applications, among them are:

(i) Manual intervention which is strongly dependent on operator skills, causing problems with architecture reproducibility;

(ii) The use of toxic organic solvents which are required in most of conventional techniques and which can cause adverse effects on cell adhesion and incorporation of biological agents if their removal is not complete;

(iii) The use of porogenic agents tends to limit the scaffolds sizes to a thin thickness and problems related to the dispersion of the pores due to agglomeration of particles as well;

(iv) limitations to produce different shapes, that restrict the frameworks into thin membranes or simple and uniform geometries (ALLAF et al., 2013; KIM; SHIN; LIM, 2012; LEONG; CHEAH; CHUA, 2003).

Due to these limitations, additive manufacturing technology, commonly called 3D-printing, became attractive to produce scaffolds with high complexity in macro and micro structures for use in tissue engineering. Additive manufacturing is defined as automated deposition of each 3D parts layer sequence, based on computational models, into the ultimate desired architecture, through additive layer-by-layer (HUTMACHER; SITTINGER; RISBUD, 2004; O'BRIEN et al., 2015).

The main advantages of additive manufacturing include: (i) customized design using CAD (computer aided design) models, allowing incorporation of specific data of tissue to be regenerated into scaffolds architecture; (ii) manufacturing process is controlled by computer, enabling to produce scaffolds with high precision and consistent morphological structure; (iii) fabrication of scaffolds with anisotropic structure by incorporation of different microscopic and macroscopic models in different regions in the same scaffold, being advantageous in applications where multiple cell linages are needed to tissue regeneration; (iv) favorable processing conditions that include solvent-free processes and / or porogenic agent; (v) moreover, some additive manufacturing techniques allow the incorporation of biologicals and pharmaceuticals molecules during fabrication (LEONG; CHEAH; CHUA, 2003)

Among the 3D printing techniques, the most industrially diffused technologies that can be applied to manufacture scaffolds with specific controlled geometry are:

- Selective Laser Sintering (SLS) - Metals, ceramics and bulk polymers compounds. Parts are produced with high accuracy, good mechanical strength and broad range of bulk materials. Materials can be trapped in small inner holes is difficult to be removed, in addition biodegradable materials may be degraded in the chamber;

- Stereolithography (SLA) - Photopolymer resins. Relatively easy to remove support materials and relatively easy to achieve small feature. Limited by the development of photopolymerizable and biocompatible, biodegradable liquid polymer material;
- Fused Deposition Modeling (FDM) - Some thermoplastic polymers/ceramics. Low cost. Elevated temperatures and small range of bulk materials;
- 3DP (Three-dimensional Printing) – The "Ink" is prepared from polymer or ceramic powder. Without inherent toxic component. Weak bonding between particles and bad accuracy-rough surface (OLIVEIRA et al., 2007).

The first step to produce a scaffold by additive manufacturing technique is generating a CAD model; the second is the translation of this model into a file exchange, named STL, which serves as the standard language of mosaic; thirdly, the STL file is imported and the virtual model is sliced into horizontal layers and oriented toward optimal deposition. The generated file is called g-code, which is used for printing equipment to part manufacture (VAEZI; SEITZ; YANG, 2013).

2.2.1.1. Fused Deposition Modeling (FDM)

FDM is an AM technique in which a thermoplastic filament is melted in a head-heated connected to a carriage moving in the horizontal xy plane (Fig. 2.2.). The heated-head deposits the material through a nozzle directly on to the build platform, following a programmed path. When a layer is deposited, the platform moves down in the z direction to deposit the next layer (BOSCHETTO; BOTTINI, 2014; MOHAMED; MASOOD; BHOWMIK, 2015; ZIEMIAN; CRAWN, 2001). Different parameters can be controlled during the FDM process, such as:

- First-layer height – It affects the adhesion of printed part on the building platform;
- Layer-height – It changes the quality of final part by affecting the definition of the printing process;
- Fill density – It indicates the amount of filament that will be extruded to fill up the part.
- Fill-up-pattern – The software Slic3r® presents different fill-up patterns being 4 based in simple-geometries and 3 based in complex geometries. This parameter will determine the printing path and the way that the machine will deposit the melted filament onto the building platform;
- Deposition speed – Affect the mechanical behavior and quality of printed parts.

The combination of these parameters results in scaffolds with controlled morphology/geometry, porosity, pore size and pores interconnectivity (CHIA; WU, 2015). The key advantages of FDM to manufacture scaffolds for TE are high porosity, good mechanical strength and low fabrication cost, in comparison with another AM techniques.

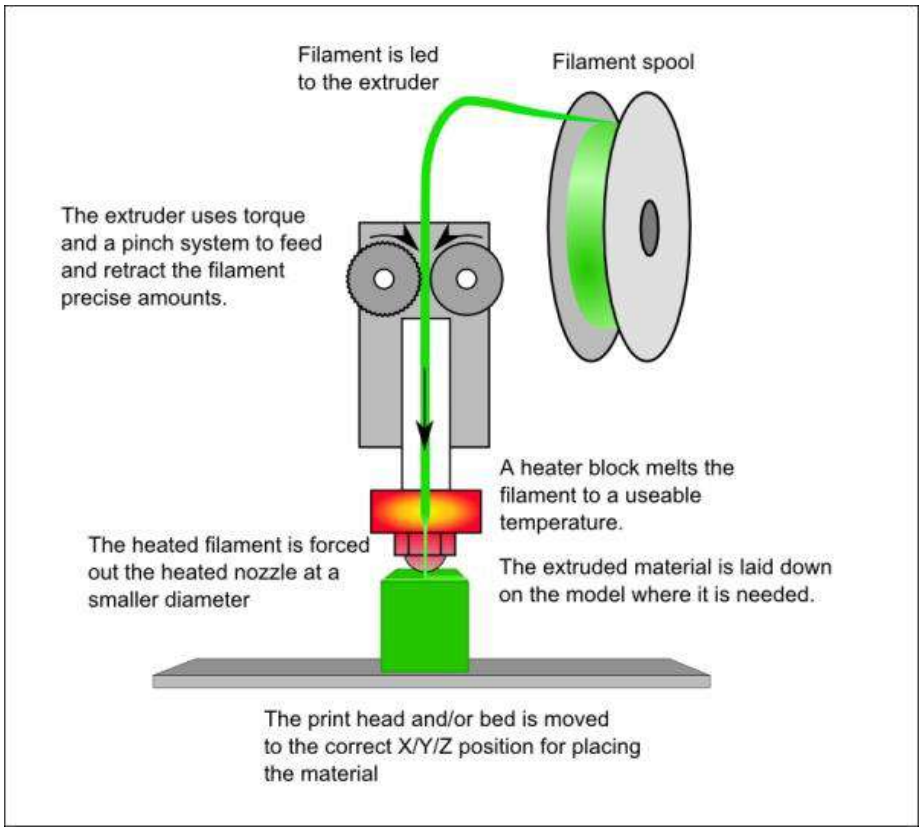

Fig 2.2. Schematic representation of an FDM machine

At the beginning, this technology was applied to produce certain objects such as toys and parts for industries. However, due to the low cost to produce 3D parts, FDM becomes attractive as a way to develop medical devices. Scaffolds manufactured via FDM present satisfactory pore reproducibility and interconnectivity, besides adjustable geometries and accuracy. It is possible to determine printing parameters, such as filament thickness, deposited layer height, deposition angle and deposition speed, and include them in g-code. These parameters have direct influence on the quality of printed part and they can be set according to the defined application (KALITA et al., 2003).

The rheology is one of the most important criteria to choose a material to FDM. Thermoplastic polymers are widely applied in this technique due to low melting temperature and the heat transfer characteristics. The selection of the material to manufacture 3D scaffolds by FDM depends, among others characteristics, on mechanical properties, processability, biodegradability and biocompatibility (HUTMACHER et al., 2007; SUSMITA BOSE; BANDYOPADHYAY, 2012). Different polymers are raw material to produce scaffolds for TE engineering, such as acrylonitrile butadiene styrene (ABS), polycaprolactone (PCL), poly(lactic acid) (PLA) etc.

Different geometries and raw materials are applied to manufacture scaffolds by FDM technique. Ceretti et al. (2017) manufactured multilayer PCL scaffolds, with different pore sizes and path height, by FDM. The authors, also, analysed the influence of different extrusion technology (filament or powder extrusion head). They evaluated the process accuracy, dimensional deviation of the parts and biological response as well. Printed parts seems to be more stable for powder extrusion in comparison with filament. Nevertheless, stability of pores was higher for parts manufactured from filament extrusion. In the biological investigation, it was observed that cells, although the hydrophobic profile of PCL, were seeded onto scaffolds grids, colonizing all the structure. They conclude that FDM was an efficient technique to produce scaffolds and it allowed to change the heated-head according the project and raw material (CERETTI et al., 2017).

Korpela et al. (2013) produced biodegradable porous scaffold from PLA, PCL, poly(e-caprolactone)/bioactive glass (PCL/BAG) composite and L-lactide/e-caprolactone 75/25 mol % copolymer (PLC) in FDM. They evaluated the compressive properties and the fibroblast cell response to the structures. It was observed that it is

possible to change compressive stiffness of scaffolds without change compressive modulus and the mechanical characteristics were completely dependent on porosity and structural geometry. Nonetheless the biocompatibility of all materials, the cell proliferation was significant higher for PLA scaffolds in comparison with the other scaffolds (KORPELA et al., 2013).

Ostrowska et al. (2016) investigated the influence of internal pore architecture on the biological and mechanical properties of PCL scaffolds produced via FDM. Scaffolds with six different geometries (angle deposition: 0°/15°/30°, to 0°/30°/60°, 0°/45°/90°, 0°/60°/120°, 0°/75°/150°, and 0°/90°/180°) were fabricated. It was observed that scaffolds had completely interconnected pore network ranging from 380 to 400 μm (0°/15°/30° to 0°/90°/180°), with porosity in the range of 50%-60%. Mechanical properties was significantly affected by the deposition angle. Cell behaviour was improved for scaffolds with 0°/15°/30° in angle deposition (OSTROWSKA et al., 2016).

Rosenzweig et al. (2015) produced large-pore (700 μm) scaffolds from acrylonitrile butadiene styrene (ABS) and polylactic acid (PLA) via FDM for cartilage and nucleus pulposus regeneration. Scaffolds were compared for cell ingrowth, viability, and tissue generation. Articular chondrocytes and nucleus pulposus (NP) cells were cultured on ABS and PLA scaffolds for three weeks. Both cell types proliferated well, showed high viability, and produced ample amounts of proteoglycan and collagen type II on both scaffolds. Both scaffolds types were mechanically stable under compressive load and the authors conclude that was possible efficiently produce scaffolds with adequate mechanical and biological properties in a simple FDM equipment (ROSENZWEIG et al., 2015).

2.2.2. PLA

PLA is an aliphatic synthetic polyester, obtained from renewable sources, widely applied in biomedical field due to its biocompatibility and biodegradability (Fig 2.3.). This polymer is produced from the polycondensation of lactic acid or ring opening polymerization of the cyclic dimer lactide (SANTORO et al., 2016). PLA is thermally stable, has low environmental impact and mechanical resistance in comparison with conventional polymers such as polyethylene, polypropylene and polyethylene terephthalate (PET), features that make it attractive to the industry. PLA is a semi-crystalline polymer with the glass transition temperature (Tg) around 55°C and melting temperature (Tm) approximately 180°C. The thermal properties of PLA could be affected by different structural parameters, such as molecular weights and composition (HAMAD et al., 2015).

PLA presents two optical forms: D-lactide and L-lactide. It is possible to regulate physical properties and the biodegradability of PLA by employing a hydroxyl acid co-monomer component or by racemization of the D- and L-isomers. The rate of degradation of PLA is dependent upon the degree of crystallinity. The biodegradability of PLA can be tailored by grafting (TYLER et al., 2016). The main product of PLA degradation, in mammal's body, is the α-hydroxy acid, which is incorporated by the carboxylic acid cycle and completely excreted. PLA is approved by Food and Drug Administration (FDA) to applications that require direct contact with biological fluids (CARRASCO et al., 2010; RASAL; HIRT, 2010).

PLA has been applied as suture, bone fixation devices, part of drug delivery system and scaffolds for tissue engineering. The relevance of this polymer for biomedical applications occurs not only for its biodegradability, but also its

biocompatibility and thermal and mechanical stability. PLA provides excellent properties at low prices in comparison to other materials (LASPRILLA et al., 2012). Several studies use pure PLA or PLA mixed with another polymer or ceramic material to produce scaffolds for tissue engineering (CARLOS; MAIA-PINTO; THIRÉ, 2016)

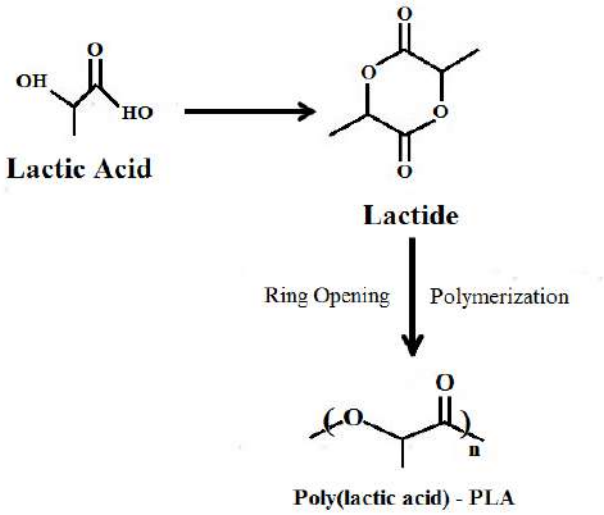

Fig. 2.3. PLA chemical structure

Almeida et al. (2013) evaluated the cytokine profile of human monocytes/macrophages in contact with 3D scaffolds with different surface properties, architecture and controlled pore geometry. Scaffolds were produced from polylactic acid (PLA), PLA/calcium phosphate glass or chitosan. Although all scaffolds supported monocyte/macrophage adhesion and stimulated cytokine production, a substantial differences between PLA-based and chitosan scaffolds was found. PLA-based scaffolds reduce the production of TNF, a pro-inflammatory protein and induced higher production of interleukin (IL)-6, IL-12/23 and IL-10, anti-inflammatory cytokines (ALMEIDA et al., 2014).

Haddad et al. (2016) designed PLA nanofibrous scaffolds by electrospinning with interconnected pores. Scaffolds were functionalized with polyallylamine to introduce amine groups by wet chemistry with subsequent covalent grafting of epidermal growth factor (EGF). The authors obtained satisfactory mechanical and structural properties. The response of Neural Stem-Like Cells (NSLCs) to PLA scaffolds was evaluated and it was possible to observe that the cells were able to proliferate on these EGF-grafted PLA substrates and remained viable up to 14 days (HADDAD et al., 2016).

Despite being widely applied to manufacture biomedical devices, PLA is a hydrophobic polymer and it does not present a variety of chemical sites to allow cell interaction and it is considered a low bioactivity polymer. Accordingly, it is necessary to improve its surface properties to allow cell interactions, improving the potential for bone tissue engineering (SERRA et al., 2013).

.

2.3. Surface modification – Mussel inspired method

Bioactivity is a key to the success of cells interaction with the biomaterial surface (Fig 2. 4). The chemistry of a surface will modulate the specific bind between biomaterials and receptors in cell membrane, such as integrin, and cell signalling process. Consequently, the surface chemistry act controlling the phenotype and function of cells (ROACH et al., 2007). Most of the synthetic materials, that are commonly applied to manufacture scaffolds for tissue engineering, do not possess adequate surface chemistry to allow cell binding/attachment. In these cases, the surface modification is an alternative to improve the biomaterial bioactivity (DOMINGOS et al., 2013; IKADA, 1994).

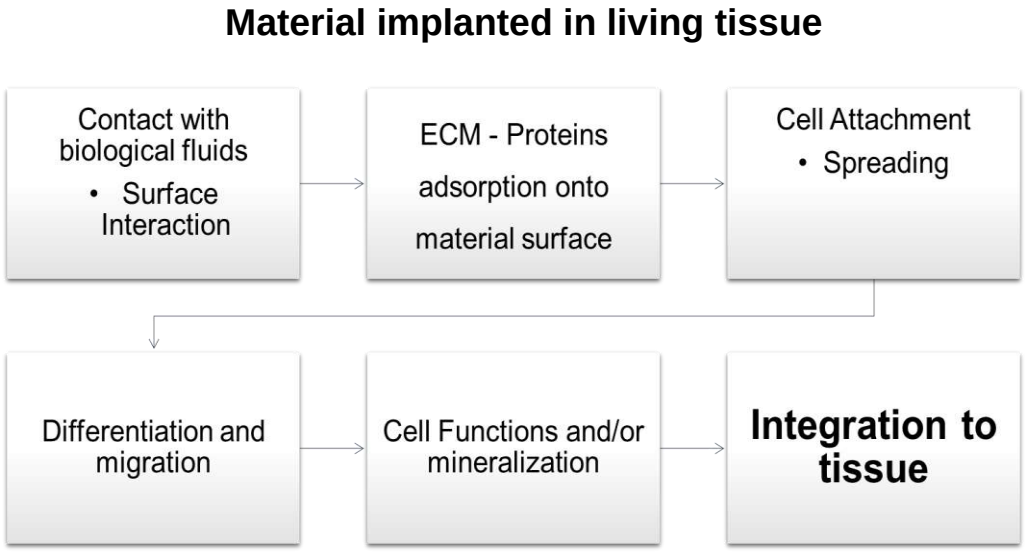

Fig. 2.4. Steps of biomaterial-tissue interaction.

A wide range of biomolecules, such as proteins or growth factors, can be immobilized onto the surface of biomaterials for bone TE to improve its bioactivity. Proteins have domains in their structures that can bind with integrin, accelerating cell attachment and spread. Different methods are applied to immobilize proteins onto a polymeric surface such as adsorption via electrostatic interactions, ligand–receptor pairing, and covalent attachment. The covalent immobilization of proteins offers several advantages by providing the stable bond between biomolecule-surface (GODDARD; HOTCHKISS, 2007).

Collagen (Fig. 2.5.) is the most abundant protein in mammal body and is widely applied to enhance the bioactivity of biomaterials. More than 20 types of collagen can be found in the organism, being collagen type I (COL I) the major organic component of bone extracellular matrix. It has been well illustrated that the typical triple helix structure (Gly-Xaa-Yaa)n sequences) within extracted collagen type I could interact with cell surface receptors such as integrins (α2b1, α1b1, α10b1, α11b1), discoidin

domain receptors (DDR1 and DDR2), mannose receptors and osteoblast receptor. COL can regulate cell adhesion, proliferation and migration (HU et al., 2017). The immobilization of collagen on the surface of biomaterials have been applied as a way to enhance the bioactivity of surfaces for bone tissue engineering.

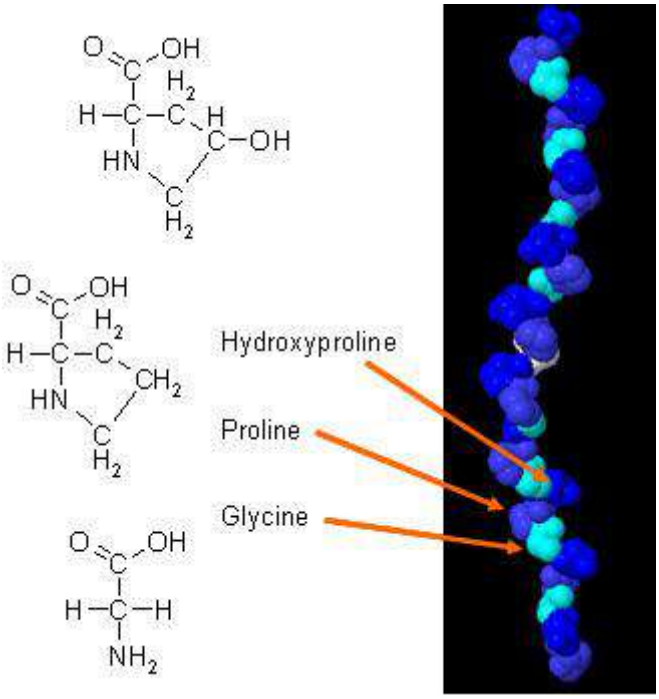

Fig. 2.5. General chemical structure of collagen

(http://proteopedia.org/wiki/images/e/e5/Collagen_%28alpha_chain%29.jpg)

Sousa et al. (2014) produced PLA scaffolds and, in order to enhance the polymer bioactivity, they treated the surface with argon plasma, followed by the acrylic acid (AAc) grafting by ultraviolet (UV) and collagen immobilization via carbodiimide chemistry. The immobilization of collagen onto the surface of PCL scaffolds brought a significant increasing in the hydrophilicity, a fundamental parameter to support the

initial cell adhesion, spreading and proliferation. It was possible to observe a further improvement in the adhesion of fibroblast (SOUSA et al., 2014).

Xiong et al. (2015) produced nanofibrous scaffolds from bacterial cellulose (BC). The scaffold was modified by laser perforation technique, in order to create macropores on the structure. To further improve its bioactivity, collagen (COL) was immobilized on the surface by solution immersion and subsequent crosslinking. The BC/COL nanocomposite was characterized and the presence of macropores and COL was confirmed by SEM and FTIR. Biological *in vitro* study demonstrated that both, macropores creation and COL immobilization improved the biological activity over BC and BC/COL (XIONG et al., 2015).

However numerous strategies have been developed to covalent bind collagen onto the surface of biomaterials to bone regeneration, such as chemical conjugation, film deposition and plasma treating (DING; FLOREN; TAN, 2016), most of the methodologies involve complex chemical compounds application which usually introduces extra toxic factors or that do not allow strong interaction between COL and the surface, leading to the removal of COL from de surface when in contact with culture medium (CHENG; TEOH, 2004; SOUSA et al., 2014; WANG et al., 2015b; YANG; BEI; WANG, 2002).

2.3.1. Mussel Inspired Method

A simple and one-step method for surface modification, based on the mussel-inspired polydopamine (PDA), was proposed by Messersmith's group (KAO et al., 2015; LEE et al., 2007) as a way to improve the bioactivity of different materials, in addition to, it works as a bridge to covalent binding biomolecules. It is known that

mussels strongly adhere to surfaces, ranging from natural inorganic materials, such as rocks, and organic materials such as fish skins, to synthetic materials, even in wet marine conditions. Fig.2.6 shown the way that mussels adhere on the surface. This occurs due to the reactive catechol containing compound 3,4-dihydroxyphenyl-L-alanine (DOPA-K) and lysine, motif found in Mefp-5 (*Mytilus edulis* foot protein 5), one of the proteins in the abyssal adhesive plaque of the mussel.

Fig. 2.6. Mussel secret proteins that allow them to adhere in a variety of surfaces. (https://www.nsf.gov/news/news_summ.jsp?cntn_id=100318).

The catecholamine molecule, dopamine (DA) (Fig. 2.7.), a neurotransmitter secreted from nerve endings contains the same catechol functional group as the chain of DOPA-K residues which can be applied in the same way as Mefp-5 (KIM et al., 2013; YEH et al., 2015). DA has the ability to self-deposition onto hydrophobic or hydrophilic surfaces via rearrangement of its molecules, in the presence of oxygen and in a weak

alkaline buffer solution (pH > 7.5) (Fig. 2.8.) (KIM et al., 2013; TRIPATHI et al., 2016). The layer that is formed on the surface is called as polydopamine (PDA). The PDA deposition has been used successfully as anti-corrosion layer for microtribology, to enhance dispersion for electrocatalysis, as fouling-resistant membrane materials for water purification. Moreover the PDA layer can act increasing the bioactivity of surfaces, promoting better cell attachment and spread, since it is a major component of melanin, a biomolecule widely distributed into human body (DING; FLOREN; TAN, 2016). PDA is, also, pointed as a platform to enhance the adhesion of different proteins and biomolecules onto the surface, not only to promote strong interaction between protein-surface, but also to prevent possible protein denaturation, which acts increasing cell adhesion (KU et al., 2010; MADHURAKKAT PERIKAMANA et al., 2015; TSAI et al., 2011).

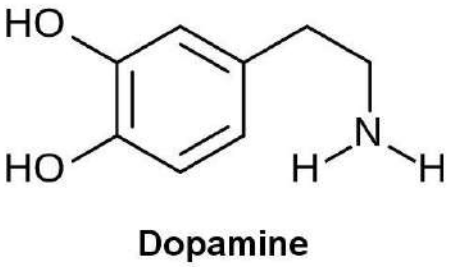

Fig.2.7. Dopamine chemical structure

Ku and Park (2010) reported the development of a nanofibrous scaffold produced from PCL and coated with PDA to enhance the adhesion, proliferation and phenotypic maintenance of human umbilical vein endothelial cells (HUVECs). PCL fibers with 700 nm were prepared by electrospun and then coated PDA by direct immersion. The authors evaluated the PDA immobilization on the surface of PCL using SEM, Raman spectroscopy, and water contact angle measurements and they observed

that a PDA layer was created uniformly on the surface. PDA coated nanofibers were cultured with HUVECs and the results were compared to HUVECs cultured onto unmodified PCL fibers and gelatin-coated PCL fibers. PDA layer helped to highly enhance adhesion and viability, increasing stress fiber formation, and positive expression of endothelial cell markers. The authors suggested that PDA coating is a promising and effective strategy for vascular tissue engineering that requires efficient endothelialization of graft surfaces (KU et al., 2010).

Tsai et al. (TSAI et al., 2011) evaluated the effect of PDA coating on the rabbit chondrocytes interaction to polycaprolactone (PCL), PLA, poly(lactic-co-glycolic acid) (PLGA) and polyurethane (PU) films for articular cartilage TE. The immersion of the samples in PDA solution for only 4 minutes was enough to increase cell adhesion and growth in comparison with uncoated surfaces. The surfaces that were treated with PDA had the capacity to hold more fibronectin, a serum adhesive protein, than uncoated surfaces. PU 3D-scaffolds were also treated with PDA and the cell proliferation and glycosaminoglycan deposition was higher for coated scaffolds in comparison with the uncoated group. Kao et al. also show that PDA strategy could be applied to regulate human adipose-derived stem cells (hADSCs) behaviour which were cultivated on to PLA 3D-printed scaffolds (KAO et al., 2015).

Rim et al. (2011) produced poly(l-lactide) (PLLA) nanofibers by electrospun and promote the functionalization with PDA, to regulate adhesion, proliferation and differentiation of human mesenchymal stem cells (hMSCs). PDA-PLLA fibers modulated hMSC responses. Initially, the PDA layer enhance significantly the adhesion and proliferation of hMSCs in comparison with cells cultured onto uncoated PLLA. The ALP activity, a early stage bone marker, of hMSCs cultured on PDA-PLLA was higher than on PLLA, as well as calcium deposition. hMSCs cultured on PD-PLLA showed

up-regulation of genes associated with osteogenic differentiation as well as angiogenesis. The authors conclude that the bio-inspired coating can be used as a simple technique to enhance the bioactivity of PLLA fibers, enhancing the specific responses of hMSCs (RIM et al., 2012).

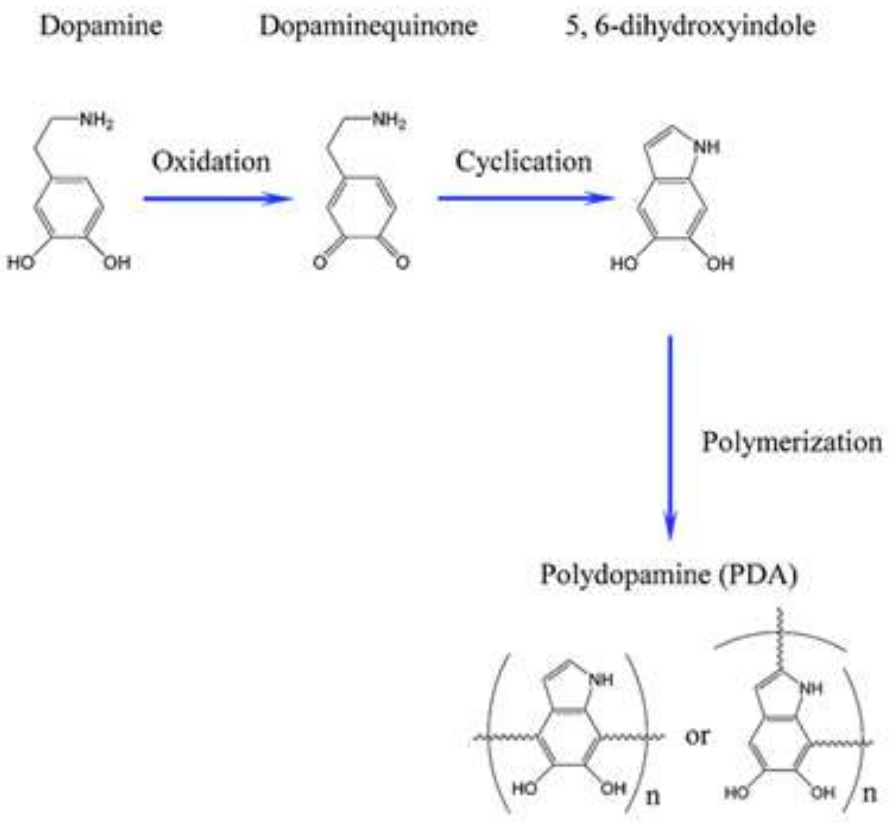

Fig. 2.8. Rearrangement of DA molecules into PDA.

3. Goals

This study aimed to produce 3D printed-PLA scaffolds via FDM, with physico-chemical and surface properties suitable to applications in bone tissue engineering. For this, scaffolds with different geometries were studied. Besides, a simple method to promote surface modification with PDA and COL I was employed, in order to enhance the bioactivity and osteogenesis as a response to the coatings.

3.1. Specific goals

- To design and manufacture PLA scaffolds with different strut space, in order to create different geometries/pore sizes and porosities;
- To improve the surface of PLA scaffolds via modification based in the mussel-inspired model, followed by COL I immobilization;
- To evaluate the accuracy of FDM to produce PLA scaffolds by dimensional deviation of printed parts from de virtual model and evaluate the reproducibility of the technique;
- To evaluate physical and mechanical properties of PLA scaffolds manufactured by FDM;
- To characterize the surfaces that were obtained by the modification with PDA and COL I;
- To study porcine Bone Marrow Stem Cells (MSCs) behaviour as a response to different coatings in short and long term *in vitro* cell culture;
- To study MSCs behaviour as a response to variation of strut space in long term *in vitro* culture.

4. Materials and Methods

4.1. Materials

White PLA filament was purchased from E-Sun (China), code Batch 20140620-1, with 1.75mm of diameter. NaOH was purchased from Vetec Química Fina Ltda. MES buffer, Dopamine Hydrochloride 98%, 1-(3-Dimethylaminopropyl)-3-ethylcarbodiimide (EDC) and N-Hydroxisuccinamide (NHS) were purchased from Sigma Aldrich. Collagen type I rattail was purchased from Corning (Fischerscientific).

4.2. Design and Fabrication of PLA scaffolds

At first, the g-code was designed with first layer height (0.22 mm); layer height (0.1 mm); fill-density (50%), fill-up pattern (rectilinear) and raster-angle (0°-90°). From these parameters, the first layer was not adhering to the building platform and parts were being produced with low quality.

Tetragonal honey-comb like porous scaffolds (3.9 mm in z, 6.3 x 6.3 mm in x and y), with 0/90° on layer-down-pattern, 0.3 mm for layer high and 0.8 mm, 1 mm or 1.2 mm of strut spacing were designed using SolidWorks® software (Fig. 4.1) in order to create matrices with pore size in range of 500µm, 700 µm and 900µm, respectively. The models were saved as .STL file. The printing parameters were defined following the profiles for slicing in the software Slic3r®. Then the .STL file was sliced to create the g-code, which was exported to a 3D Cloner® (Microbrás, Brazil) printer (Fig. 4.2.). Scaffolds were constructed from PLA commercial white filament. PLA filament was extruded at 220°C, 60 mm/s, through a nozzle, with 0.3 mm in diameter and deposited

layer-by-layer. Porous scaffolds were namely as P500, P700 and P900, as a function of strut spacing.

4.3. Surface Modification

Scaffolds were hydrolyzed with sodium hydroxide (NaOH) 0.1M solution, constant agitation at 65°C for 45 minutes. Scaffolds were washed three times, with de-ionized water, to eliminate eventual residues of NaOH. This treatment was applied to remove non-projected filaments that arise as a result of the printing path. The hydrolysis also promotes the break of esters bonds, exposing carboxylic acid on the surface, improving cell adhesion.

PLA scaffolds, previously hydrolyzed, were soaked into dopamine hydrochloride (2mg/ml) solution prepared with MES buffer, pH 8.5, under constant agitation (120rpm), for 24 hours, at room temperature (1 scaffold per 2ml of DA solution) (KAO et al., 2015). Scaffolds were rinsed to remove non-coupled DA molecules and dried at room temperature. Samples were namely as PLA (uncoated scaffolds) and PLA DOPA (PDA coated scaffolds)

PLA and PLA DOPA scaffolds were soaked into COL I rattail solution [100µg/ml] containing EDC (10mM) and NHS (25mM) in ultra-pure water (1 scaffold per 2ml of COL I solution) for 48h at 4°C, followed by several rinses with de-ionized water (YU; WALSH; WEI, 2014). Scaffolds were dried at room temperature. Samples were namely as PLA COL (PLA coated with COL I) or DOPA COL (PLA DOPA scaffolds coated with COL I).

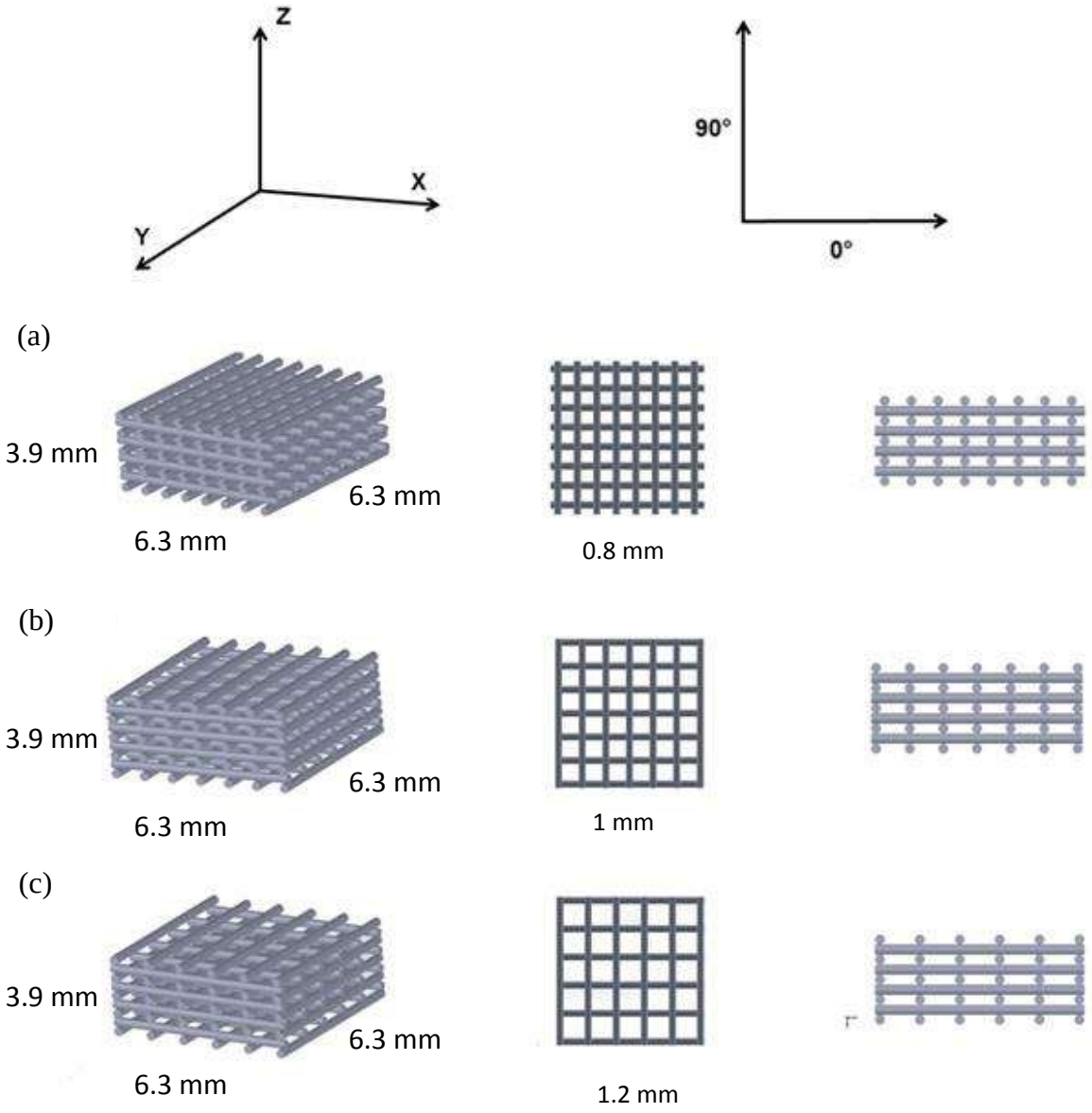

Fig.4.1. Virtual model of PLA scaffolds (a) P500, (b) P700 and (c) P900

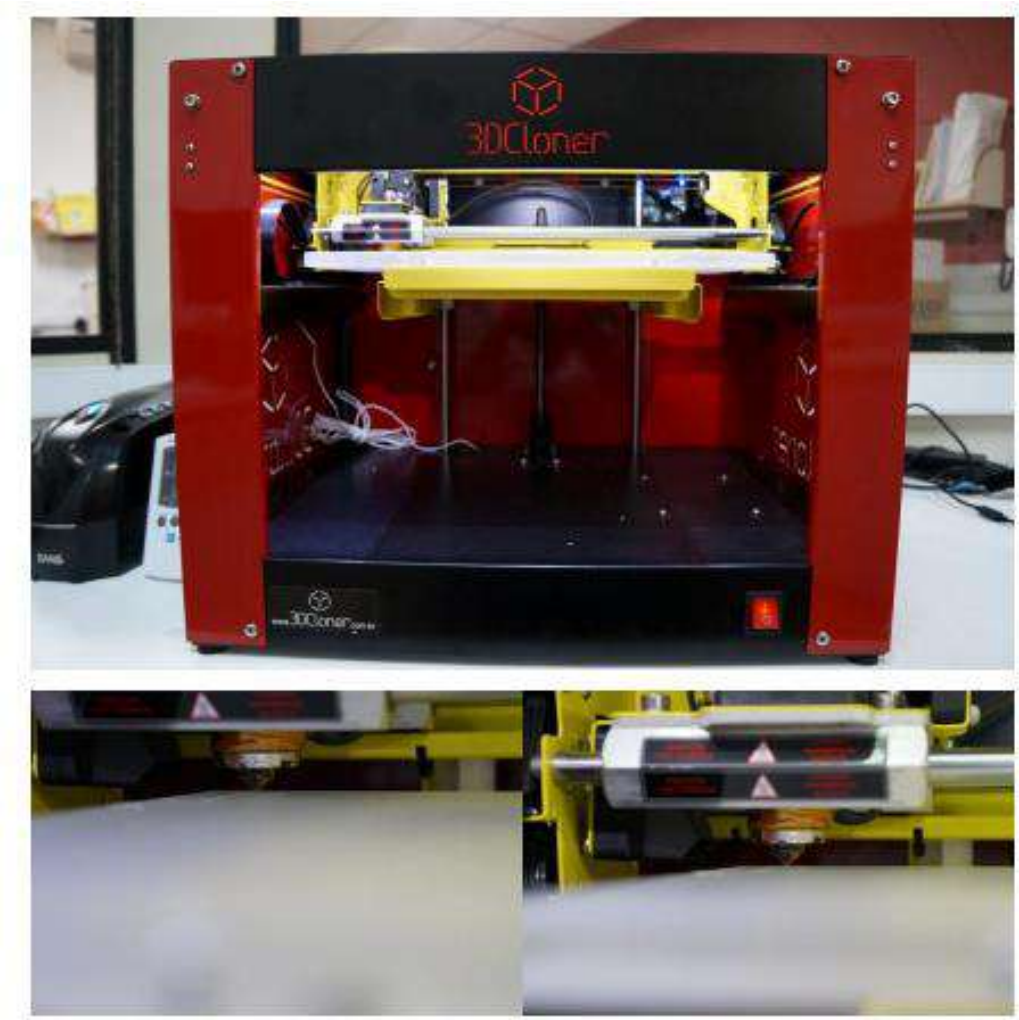

Fig. 4.2. Commercial printer 3D Cloner ® (Microbrás)

4.4. Dimensional Deviation (Dd) of Printed Parts

Five specimens (n=5) of PLA scaffolds were measured with a digital caliper (Vonder®) in high (z), width (x) and depth (y) to evaluate the dimensional deviation of printed parts in comparison with the designed model. After measurements, values were obtained using the Equation:

$$Dd = \frac{(x - x')}{x'} * 100$$

where x corresponds to the measured value for the axis and x' corresponds to the projected value for the axis.

4.5. Porosity

Scaffold porosity was measured by the indirect method based on Archimedes' Principle, according ASTM F2450-10. The apparent density of scaffolds (n=5) was obtained by ethanol immersion, using the Equation:

$$\rho a = Ms * \frac{\rho l}{(Ms - Mm)}$$

where ρa is the apparent density of each part, ρl is the ethanol density (0.789 $g.cm^{-3}$), Ms is the wet weight each part and Mm is the weight of the parts soaked in ethanol. From ρa value was possible to obtain the pore volume using the Equation:

$$Pv = V - (\frac{Ms}{\rho a})$$

where Pv is the pore volume, V is the volume of each part (considering scaffolds as cubes with z, x and y axis), ρa is the apparent density of each part and Ms is the wet weight each part. Porosity was measured using the Equation:

$$P = \frac{Pv}{V} * 100$$

where P is the porosity, Pv is the pore volume and V the volume of scaffold.

4.6. Compressive tests

Mechanical properties of 3D printed PLA scaffolds under compressive load were measured using a universal testing machine Zwick Z005, with a 2.5 kN load cell and cross head speed of 1 mm/ min. Samples were loaded until 30% of strain.

4.7. XPS analysis

X-ray photoelectron spectroscopy (XPS) was performed using a VG Scientific Escalab MKII system (VG Scientific, U.K.) under ultra-high vacuum conditions using Al K-alpha X-rays (1486.7 eV) and analyser pass energies of 200 eV for the survey spectra (20 scans) and 20 eV for the C1s core-level region (60 scans). The core-level was fitted using the system software and the data were analysed using CASA® software. The binding energies were referenced to the hydrocarbon component C1s (C-C; C-H) level set at 284.6 eV.

4.8. Atomic Force Microscopy analysis

Intermittent contact mode images of 3 samples (for each group) were performed using an Asylum MFP-3D AFM. Root mean square roughness (RMS roughness) values were obtained from 20 µm x 20 µm topographic images using the software Gwiddyon 2.49.

4.9. Collagen quantification

Total collagen content on to the surfaces was determined by measuring the hydroxyproline content. Each sample was digested with papain (125 $\mu g.ml^{-1}$) in 0.1 M sodium acetate, 5 mM L-cysteine–HCl, 0.05 M ethylenediaminetetraacetic acid

(EDTA), pH 6.0 (all from Sigma–Aldrich) at 60ºC and 10 rpm for 18 h. Samples were, then, hydrolysed at 110 °C for 18 h in concentrated HCL solution (38 w/w%) and assayed using a chloramine-T assay with a hydroxyproline-to-collagen ratio of 1: 7.69.

4.10. Cell Culture

Bone marrow derived mesenchymal stem cells (MSCs) were obtained from the femoral shaft of 4 month old pigs and expanded according to a modified method for human MSCs (VINARDELL et al., 2009). Cells were cultured in high-glucose Dulbecco's modified Eagle's medium GlutaMAX (hgDMEM) supplemented with 10% v/v of fetal bovine serum (FBS), penicillin (100U.ml^{-1}) /streptomycin (100µg.ml^{-1}) (all Gibco Biosciences, Dublin, Ireland) and 2.5 µg.ml^{-1} amphotericin B (Sigma–Aldrich, Dublin, Ireland) – XPAN mediun - at 37°C, 20% pO2. Cells were trypsinized, counted, seeded at density of 5.10^3 cells cm^2 in 175cm^2 triple flasks (Thermo Fisher Scientific) and cultured in XPAN medium to passage 2.

4.11. *In vitro* culture conditions

Before cell culture, scaffolds were sterilized by ethylene oxide for 24 hours. To seed cells, an agarose mould was manufactured in order to improve the efficiency of seeding and the retention of cells (Fig. 4.3). Scaffolds were placed inside the mould and were seeded with a drop of 150 µl containing 5x10^5 cells. The efficiency of cells seeding, cell viability, metabolic activity and attachment in PLA, PLA COL, PLA DOPA, and DOPA COL scaffolds were conducted into XPAN medium. The osteogenic culture condition applied in this study is defined as cells culture in a osteogenic medium

(OM) consisting high-glucose Dulbecco's modified Eagle's medium GlutaMAX (hgDMEM) supplemented with 10% v/v of fetal bovine serum (FBS), penicillin (100U.ml^{-1}) /streptomycin (100µg.ml^{-1}) (all Gibco Biosciences, Dublin, Ireland) and 2.5 µg.ml^{-1} amphotericin B (Sigma–Aldrich, Dublin, Ireland), 0.5% of dexamethasone, 1% of β-Glicerolphosphate and 0.029% of ascorbic acid (Sigma Aldrich) at 5% pCO_2. To evaluate the potential of MSCs to differentiate, cells were cultivated in Low Glucoses Dulbecco's Modified Eagle Medium (lgDMEM) supplemented with 100 U ml^{-1} penicillin/100 l µg.ml^{-1} streptomycin (both Gibco), 10% of FBS at 37C and 5% pCO_2.

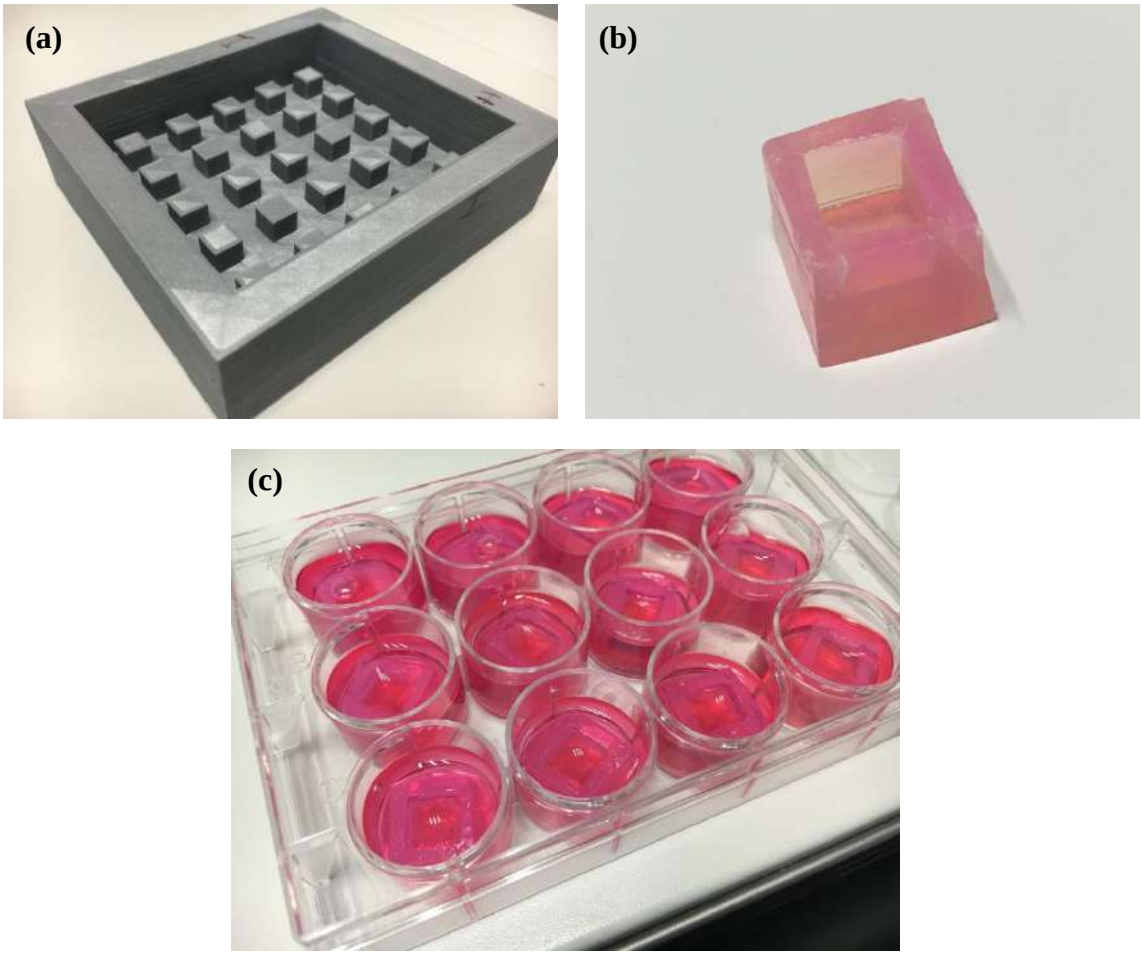

Fig. 4.3. PLA support (a) to manufacture agarose molds (b). PLA scaffolds were placed inside the mold and seeded with MSCs (c).

4.12. Evaluation of cell response to PLA scaffolds coated with PDA and COL I

The first part of the biological study was to evaluate the effect of PDA and COL I coatings in the behaviour of MSCs. For this purpose, the following methods were applied.

4.12.1.Evaluation of Cell seeding, viability, adhesion and metabolic activity

Scaffolds that were cultured with MSCs for 24 hours were digested in papain (125 $\mu g.ml^{-1}$) in 0.1 M sodium acetate, 5 mM cysteine HCl, 0.05 M EDTA, pH 6.0 (all from Sigma-Aldrich, Ireland) at 60 °C under constant rotation for 18 hours. The DNA content of each sample was quantified using the Hoechst Bisbenzimide 33258 dye assay (Sigma-Aldrich) in order to evaluate the amount of cell in each group.

Cell viability within PLA, PLA COL, PLA DOPA and DOPA COL constructs was assessed after 4 hours and 7 days of *in vitro* culture using a LIVE/DEAD® viability/cytotoxicity assay kit (Invitrogen, Bio-science, Ireland). Briefly, the constructs were washed in PBS followed by incubation in phosphate-buffered saline (PBS) solution containing 2 μM calcein AM (green fluorescence of membrane for live cells) and 4 μM ethidium homodimer-1(red fluorescence of DNA for dead cells; both from Cambridge Bioscience, UK). Scaffolds were again washed in PBS, imaged at magnification x10 with Leica SP8 confocal Scanning Confocal Microscope at 515 and 615 nm channels and analysed using LAS X Viewer® software.

Morphology of attached cells was evaluated by immunofluorescence for F-actin, vinculin and nucleus at day 1 and day 7. MSCs were fixed with 4% paraformaldehyde for 4 hours at room temperature. Each sample was blocked in 5% bovine serum albumin (BSA) for 45 minutes and, then, incubated with primary antibodies (vinculin produced

in mouse, Abcam) overnight ate 4°C. After this, the samples were permeabilized with 0.5% Triton X-100 (Sigma-Aldrich) for 30 seconds at room temperature. Following permeabilization step, the substrates were incubated, and stained with goat α mouse IgG-FITC + Rhodamine Phaloidin prepared in 2.5% BSA for 1h. To visualize F-actin and nucleus, were used rhodamine-conjugated phaloidin (Invitrogen) and 4,6-diamidino-2-phenylindole (DAPI, Sigma-Aldrich), respectively. Images were captured using a confocal laser scanner microscope (Leica SP8), after excitation at 405, 488 and 543 nm wavelengths for blue, green and red channels, respectively.

Metabolic activity of MSCs in response to PLA, PLA COL, PLA DOPA, and DOPA COL scaffolds was evaluated using AlamarBlue® assay. Fluorescence intensity of AlamarBlue® (Invitrogen) was directly proportional to the rate of metabolic activity of viable cells on to the substrates at days 0, 1, 2 and 7.

4.12.2. Evaluation of ECM deposition and Biochemical analysis

Cell ingrowth onto PLA and DOPA COL scaffolds was assessed at day 3, 7, 10 and 14 by optical microscopy.

The biochemical content of PLA and DOPA COL constructs were analysed at week 3 of *in vitro* culture. Prior to biochemical analysis, constructs were washed in PBS, weighed and frozen for subsequent assessment. Each construct was digested with papain (125 $\mu g.ml^{-1}$) in 0.1 M sodium acetate, 5 mM L-cysteine–HCl, 0.05 M ethylenediaminetetra-acetic acid (EDTA), pH 6.0 (all from Sigma–Aldrich) at 60ºC and 10 rpm for 18 h. Total collagen content was determined by measuring the Hydroxyproline content, using a Hydroxyproline-to-collagen ratio of 1:7.69. To calcium

quantification, constructs were digested in 1M hydrochloric acid at 60ºC and 10 rpm for 18 h. The calcium content was determined using a Sentinel Calcium kit .

Alkaline phosphatase activity on PLA and DOPA COL scaffolds cultured into Low Glucose medium was measured at week 3. The supernadant of each group was taken and the ALP content was determined using a SensoLyte pNNP Alkaline Phosphatase Assay Kit Colorimetric.

4.13. Evaluation of cell response to different pore size

The second part of this biological study was to evaluate the effect of different geometries in the MSCs behaviour. For this purpose, the following methods were applied.

Cell ingrowth onto scaffolds with 0.8mm, 1mm and 1.2mm assessed at day 14 and day 21 by optical microscopy.

The biochemical content of 0.8mm, 1mm and 1.2mm constructs was analysed at week 3 of in vitro culture, following the protocol presented in the item 4.12.2 for DNA assay, calcium and COL content (item 4.12.2).

5. Results and Discussion

5.1. Scaffolds Design and 3D printing

PLA scaffolds were successfully produced via FDM technique (Fig. 5.1).

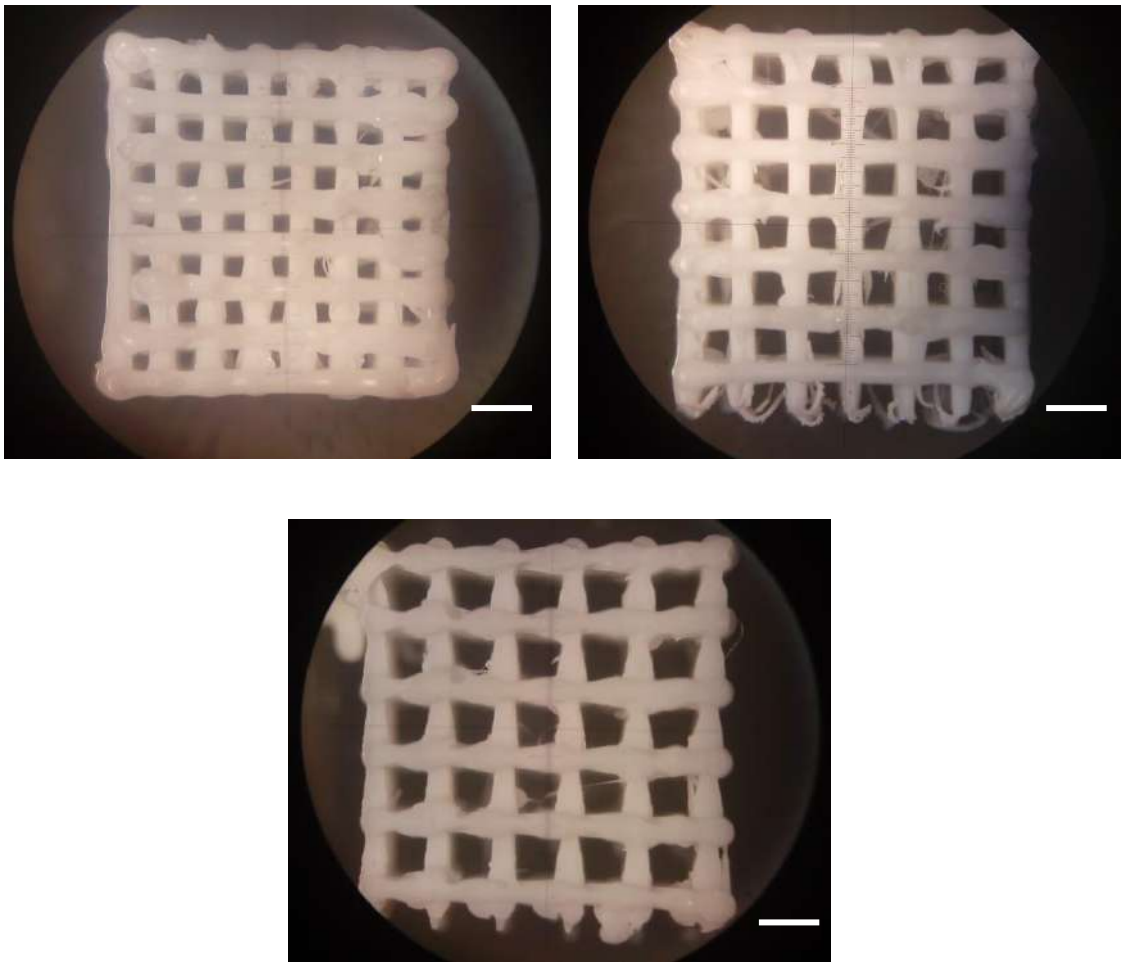

Fig. 5.1. PLA scaffolds produceb by FDM (a) P500, (b) P700 and (c) P900. Scale bar = 1 mm.

5.2. Scaffolds Characterization

To evaluate the accuracy and reproducibility of printed parts, the dimensional deviation of scaffolds was measured. Values for dimensional deviation in comparison with virtual model are shown in Fig. 5.2. Printed scaffolds showed a small positive dimensional deviation in comparison with the designed CAD model (Fig. 5.2). This difference between virtual model and printed part can occur due to the printed path, a strategy to facilitate the printing and to reduce the material waste. When the CAD model is converted into a .STL file it is sliced to generate the layers; the software then creates a path that tends to generate greater material savings and faster construction of each piece. However, when the nozzle changes trajectory during the printing process it can bring on a sudden break in the printing line with the displacement of small amounts of molten material, changing the part dimensions in the x, y and z directions (Fig. 5.3) (MOHAMED; MASOOD; BHOWMIK, 2015). The printing path is considered a deposition strategy regarding the way that the extruder nozzle travels, tracing the geometry of each layer (ZIEMIAN; CRAWN, 2001).

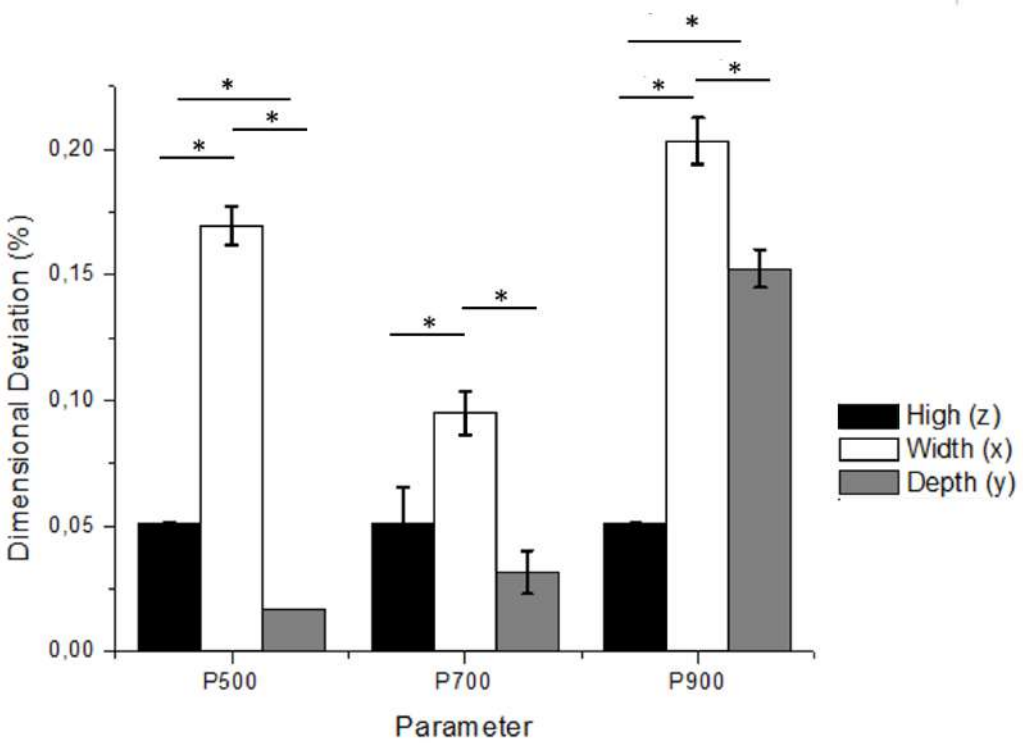

Fig. 5.2. Dimensional deviation of Printed parts. Significance: *P < 0.05

Tetragonal pores were projected to attend the ideal pore size for bone regeneration and vessels growth (Fig.5.1). The pore size was measured as the diagonal of the surface square (Table 5.1). Scaffolds were designed with two different ranges of pores, as shown in Fig.4.1. The porosity of PLA scaffolds with different strut spacing is presented in Table 5.2. As expected, the strut spacing affected the pore size and porosity of printed scaffolds; higher strut spacing present higher porosity in comparison with smaller strut spacing. The pore structure and the porosity are essential to produce successful scaffolds for tissue regeneration. Scaffolds must possess open-pore geometry with a highly porous surface and microstructure to be effective in cell culture by enabling nutrient and oxygen flow and to allow cell survival trough the material (OSTROWSKA et al., 2016). The highly porous microstructure with interconnected porous networks is critical in ensuring spatially uniform cell distribution, cell growth, proliferation and migration. In addition to porosity, the pore size is important to

determine the cell behaviour to the scaffold (HABIB et al., 2016; LEONG; CHEAH; CHUA, 2003; LOH; CHOONG, 2013; MURPHY; HAUGH; O'BRIEN, 2010) (LEONG; CHEAH; CHUA, 2003; MURPHY; HAUGH; O'BRIEN, 2010).

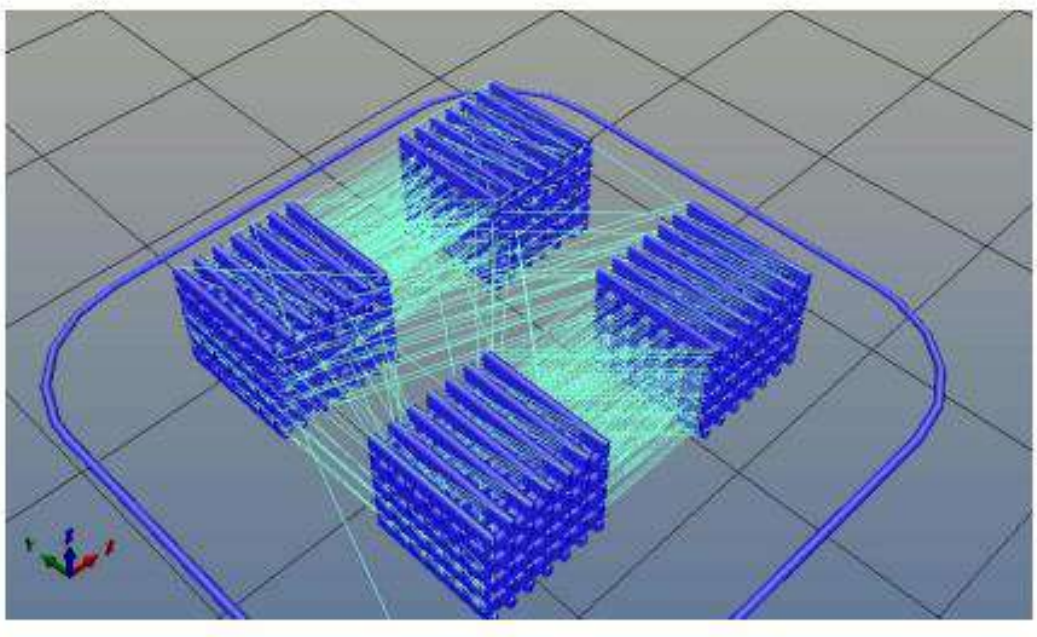

Fig. 5.3. 3D model of designed scaffolds indicating the printing path

Table 5.1. Pore sizes of virtual model and printed scaffolds

Parameter	**Projected Pore – xy (µm)**	**Projected pore – z (µm)**	**Pore size – xy (µm)**	**Pore size – z (µm)**
P500	300	500	250 ± 5	530 ± 120
P700	300	700	240 ± 10	680 ± 20
P900	300	900	270 ± 30	940 ± 187

Table 5.2. Properties of PLA scaffolds produced by FDM technique

Parameter	P500	P700	P900	Cancellous bone
Porosity (%)	55 ±1.12	60 ± 1.5	66 ± 0.34	30-90
Compressive Strenght (MPa)	13.25 ± 1.6	9.47 ± 0.48	5.75 ± 0.27	2 – 12
Elastic point (GPa)	0.52 ± 0.1	0.40 ± 0.006	0.46 ± 0.065	0.05 – 0.5

Values for compressive strength and Elastic point were presented in Table 5.2. The strut spacing affects directly the mechanical behaviour of PLA scaffolds under compressive load. Scaffolds P900 presented compressive strength of 5.75 ± 0.27 MPa, scaffolds P700 presented compressive strength of 9.47 ± 0.48 MPa and scaffolds P500 presented compressive strength of 13.25 ± 1.60 MPa. The Elastic point for scaffolds with different porosities does not present significant difference between group.

The stress - strain curves for all scaffolds groups are presented in Fig. 5.4. The curve for scaffolds P500 shown a linear elastic phase, in other words, this section represent the capacity of scaffolds to resist a compressive force without structure deformation (Figure 5.4 a). The second region of this curve is the plateau, which corresponds to the collapse of pore network. Since our scaffolds have highly interconnected porosity, this region is larger than the elastic phase (GIBSON, 2005; MOHAMED; MASOOD; BHOWMIK, 2015). Basically, the same behaviour for the curves can be observed by scaffolds P700 and P900. Since porosity directly affect the

mechanical behaviour (MOHAMED; MASOOD; BHOWMIK, 2015) the difference presented by each stress strain curve can be attributed to the difference in strut spacing that creates different pores sizes and surface areas.

Bone tissue presents compressive strength in the range of 2-12 MPa and Young's modulus in the range of 0.05-0.5 GPa (HUTMACHER et al., 2007). The maximum compressive strength and Elastic point obtained for PLA scaffolds shows that the designed model allowed to produce parts with mechanical properties in the same range of cancellous bone, as observed in Table 5.2. These results are compatible with those found by Souness et al. (2017) that evaluated scaffolds with different geometries: orthogonal structures (0/90°); diagonal structures (45/135° or 60/120°) and porous cylindrical scaffolds. The authors observed that scaffolds with lower levels of porosity presented highest compressive yield strengths and they conclude that the 0/90° geometry was the optimum for mechanical properties, pore size and diffusion coefficient, that is about the potential to delivery nutrients and oxygen to the bulk (SOUNESS et al., 2017).

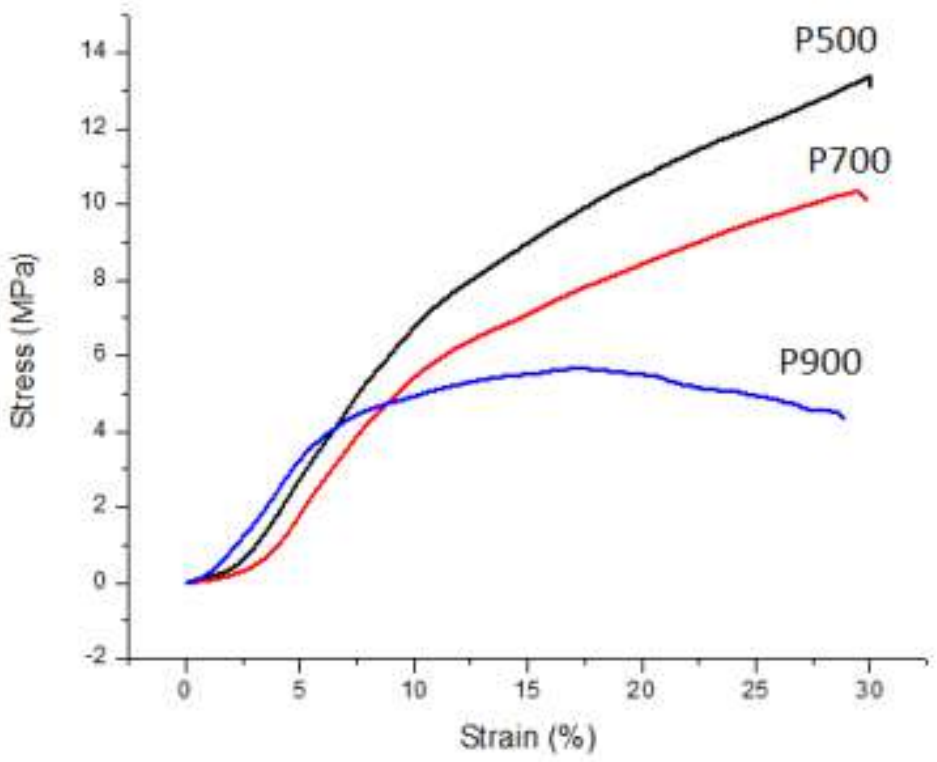

Fig. 5.4. Stress-Strain curves of PLA scaffolds with (a) P500, (b) P700 and (c) P900 under compression load to 30% of strain.

5.3. Surface Modification

Since PLA has low bioactivity, a surface modification inspired in the way that mussels can strongly adhere in a broad range of materials, was applied on to the polymer surface. In this method, Dopamine (DA), a neurotrasmissor with the same chemical structure as the protein *Mytilus Edulis Foot 5 r*esponsible for mussel adhesion, in the presence of oxygen and specific alkaline pH (8.5) undergo an oxidative rearrangement and cyclization, forming the intermediate products 5,6-dihydroxyindole (DHI) and 5,6-dihydroxyindole-2- carboxylic acid (DHICA). The rearrangement and covalent binding of these intermediate molecules presents, as a consequence, monomers

yields black-coloured in an initially colourless solution, in other words scaffolds produced with white PLA filaments become soft brown after 24 soaked in DA solution (Fig.5.5). This rearrangement in DA molecules is commonly called oxidative polymerization and the immobilized layer receives the name PDA (KIM et al., 2013). This layer enhances the bioactivity of materials and works as a platform for covalent immobilization of proteins and other biomolecules, such as COL I, one of the most abundant protein in bone matrix (TEIXEIRA et al., 2017).

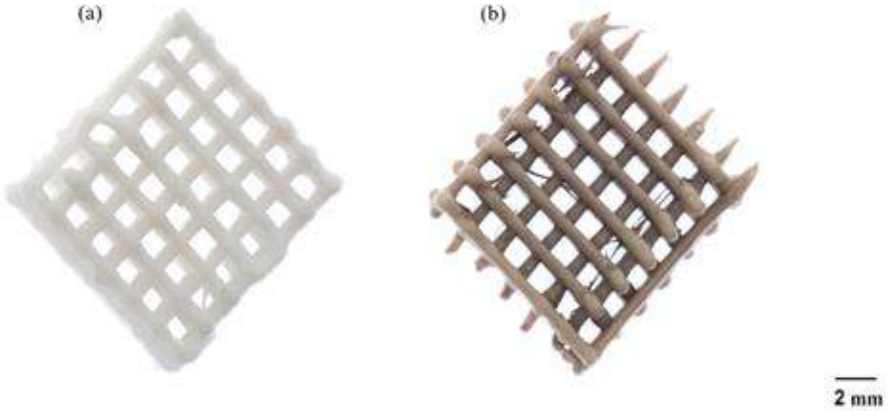

Fig.5.5. White PLA scaffolds (a) were soaked in DA solution (2 mg/ml) for 24 hours and shown a dark colour (b).

The XPS analysis focused on C1s, O1s and N1s. These regions were chosen based on the polymer atomic composition, as the composition of PLA scaffolds consist, mainly, of carbon and oxygen (LASPRILLA et al., 2012). Changes in the surface spectra were observed as function of coating (Table 5.3) and the deposition of PDA and COL is supported by the XPS C1s, O1s and N1s high resolution spectra (Fig. 5.6). After the surface modification with PDA, it could be observed a decrease in C1s from 81.17% to 73.45%. The same behaviour for carbon distribution was observed by Cheng et al. (2016) (YU et al., 2017) for PCL scaffolds immobilized with PDA. However, a small

increase in the oxygen content could be observed for scaffolds after PDA coating. As expected, an increase in N1s amount occurred when PLA scaffold were modified with PDA or with COL (CHENG et al., 2016; KAO et al., 2015; STEEVES et al., 2016). The nitrogen concentration in scaffolds coated with PDA was slightly higher (5.19%) in comparison with scaffolds coated with Col (4.06%). The overlap of PDA and COL resulted in the increase of N1S from 0% (PLA scaffold) to 7.52%. Although PDA, COL or overlap layers in scaffold surface, PLA was still dominant and contributed to the overall elemental composition (YU; WALSH; WEI, 2014).

Table 5.3. Surface atomic composition of PLA, PDA and COL-coated scaffolds by XPS.

Groups	**O1s (%)**	**N1s (%)**	**C1s (%)**	**O/C**
PLA	16.44	0	78.77	0.2
PDA	27.18	4.11	68.71	0.4
COL*	17.1	12.6	69.2	0.25
PLA DOPA	24.04	4.42	71.53	0.34
PLA COL	16.83	4.47	77.27	0.22
DOPA COL	29.11	7.31	63.57	0.46

*Values for COL were published in (YU; WALSH; WEI, 2014)

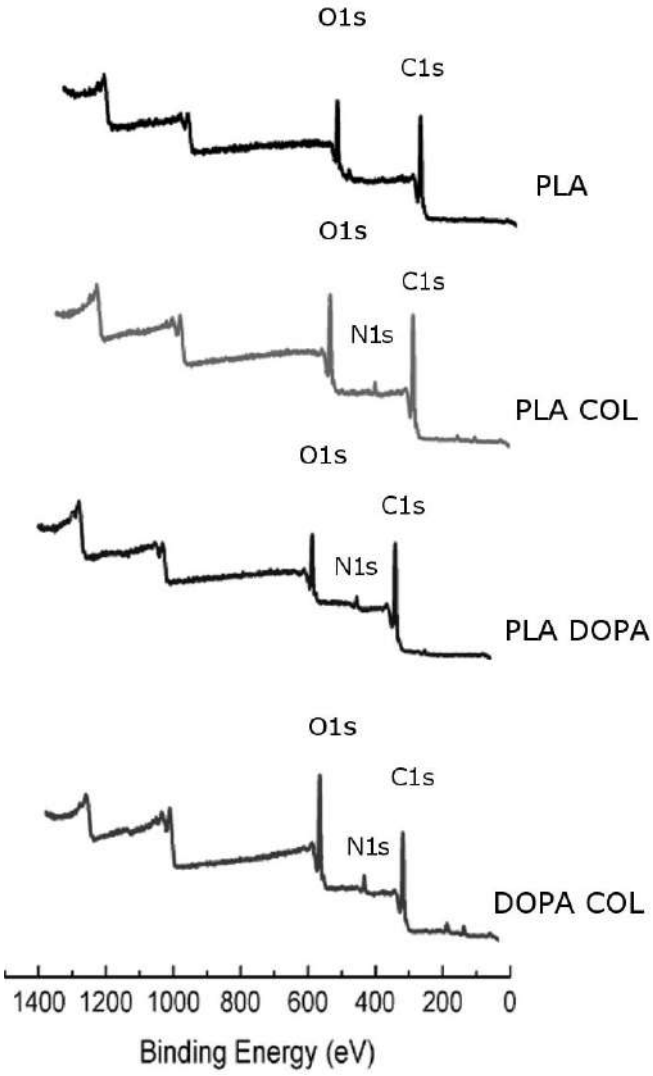

Fig.5.6. XPS survey spectra of PLA, PLA COL, PLA DOPLA and DOPA COL scaffolds

The C1s spectra of PLA can be divided into 3 main peaks (Fig.5.7). The first one at 284.1 eV was attributed to the aliphatic carbon (C-H), the second at 288.87 eV was assigned to the carbon double binding or carbon and oxygen (C=O), and peak 3 at 286.9 eV was attributed to the carbon associated with the oxygen or nitrogen (C-O, C-N). The relative area of peak 1 for PLA scaffolds was 80.79%, whereas the relative area for peak 2 and peak 3 was 7.41% and 11.79%, respectively (Table 5.4). For PLA COL scaffolds, the three relative peak areas of C1s spectra differed from uncoated PLA. The

relative area of peak 3 (C-O, C-N) increased from 11.7% to 14.4% and the relative area of peak 2 (C=O) increased from 7.41% to 11.58% (Table 5.4). For PLA DOPA scaffolds, the relative areas of peaks 1 and 2 decrease to 60.31% and 2.69% respectively, while the relative area of peak 3 increased to 30.27%. The relative area of peak 1 for DOPA COL was drastically reduced in comparison with PLA scaffolds, from 80.79% to 28.19%, while the relative area of peak 3 was substantially increased to 58.8% and may be related to the overlap of both, COL I and PDA. These changes in the surface are closely related to the coatings and, after PDA and COL I immobilization, the PLA composition was not so expressive onto scaffold surface.

Table 5.4. XPS C1s functional group percentages as a function of different coatings.

Groups	**CHx/C-NH_2**	**C = O**	**C – O/C – N**
PLA	80,791	7,4173	11,7915
PLA COL	74,004	11,587	14,409
PLA DOPA	60,319	2,69	30,2719
DOPA COL	28,19	13,001	58,809

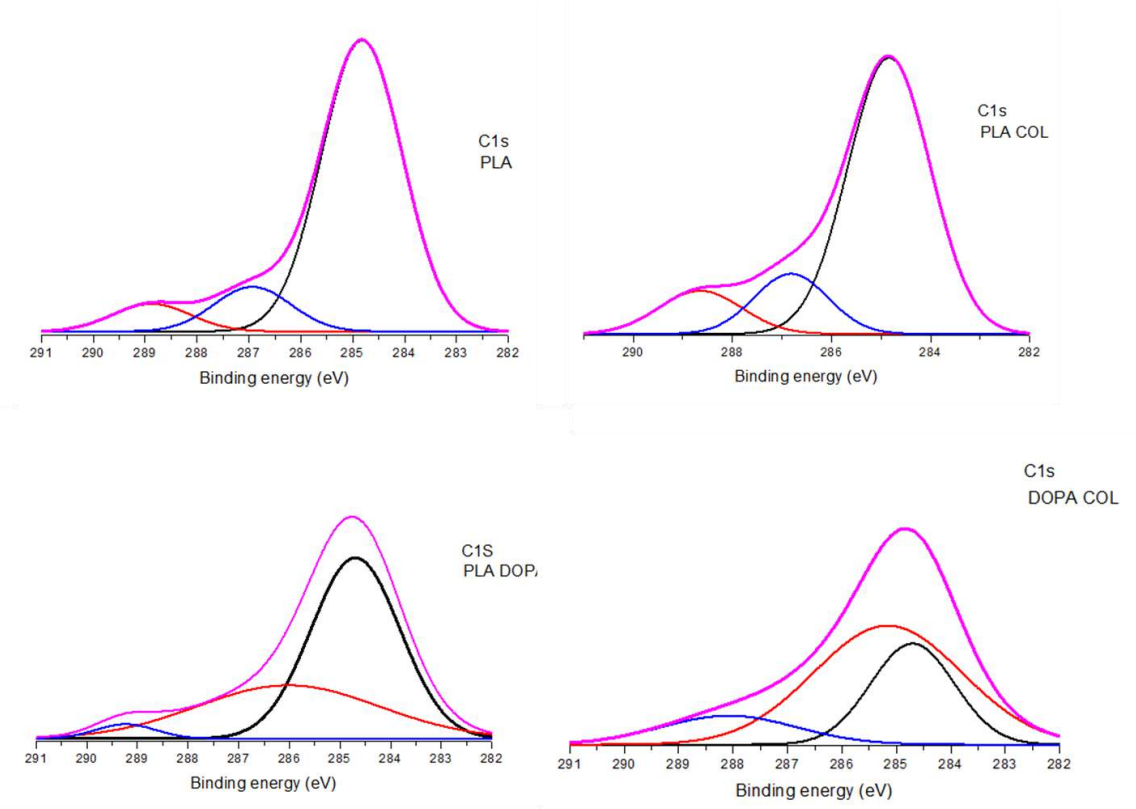

Fig.5.7. C1s spectra of PLA, PLA COL, PLA DOPA and DOPA COL scaffolds.

The differences in the relative areas of C1s deconvoluted peaks for PDA coated scaffolds is related to a large amount of hydroxyl groups of dopamine and the expressive increase in the peak 3 (C–O) area for DOPA COL. The dopamine self-polymerization like reaction promoted the reduction of hydroxyls (C-OH) to quinone species (C=O). However, those quinone species within the dopamine structure are not stable in solution, reacting with hydroxyls to form more stable PDA by anti-disproportionation reactions and can explain the decrease in relative area of peak 2 (C=O) in PLA DOPA scaffolds (HU et al., 2017). As expected, an increase in N1s amount occurred when PLA scaffold were modified with PDA or with COL (CHENG et al., 2016; KAO et al., 2015; STEEVES et al., 2016). Although PDA, COL I or overlap layers in scaffold surface, PLA was still dominant and contributed to the overall elemental composition (YU; WALSH; WEI, 2014).

Scaffolds roughness (Table 5.5) changes due to the coating composition, except for PLA coated with COL. In this case, there was no significant difference in roughness between uncoated and coated PLA scaffold. Comparing the PLA and PLA DOPA it could be observed a decrease of 60% in the surface roughness, which indicates that the DA molecules were deposited onto the PLA roughness. The subsequent coating with COL also reduced the surface roughness by 76% in comparison with uncoated PLA. Moreover, the AFM and XPS analysis showed that the PDA layer was efficiently created on to the PLA surface.

Table 5.5. Surface roughness of PLA, PLA COL, PLA DOPA and DOPA COL scaffolds by AFM.

Groups	Roughness (nm)
PLA	353.4 ± 40.25
PLA COL	337.4 ± 30.56
PLA DOPA	139.1 ± 30.16
DOPA COL	83.05 ± 13.54

Total COL on to PLA COL and DOPA COL surfaces was assessed using a biochemical assay for hydroxyproline content (Fig.5.8). The COL amount for DOPA COL scaffolds was significant higher in comparison with PLA COL scaffolds, as expected (CHENG et al., 2016).

Different methods have been proposed to promote adequate cell interaction with materials surfaces. The covalent immobilization of ECM proteins is a current approach

to surface modification since the natural ECM has several proteins that works to modulate cell adhesion and proliferation (CHENG et al., 2016). However, the methods that are currently applied to covalent immobilization of proteins cannot be applied to a variety of materials, requiring multiple complex steps to bind the molecule onto the surface (KU; LEE; PARK, 2010). The PDA layer is proposed as a simple and robust platform for covalent immobilization of proteins and other biomolecules on to the surface of printed scaffolds. As observed in Fig. 5.5, the PDA layer was easily created onto the surface of PLA scaffolds and allowed a significant increase in the total COL I immobilization, as observed in Fig. 5.7.

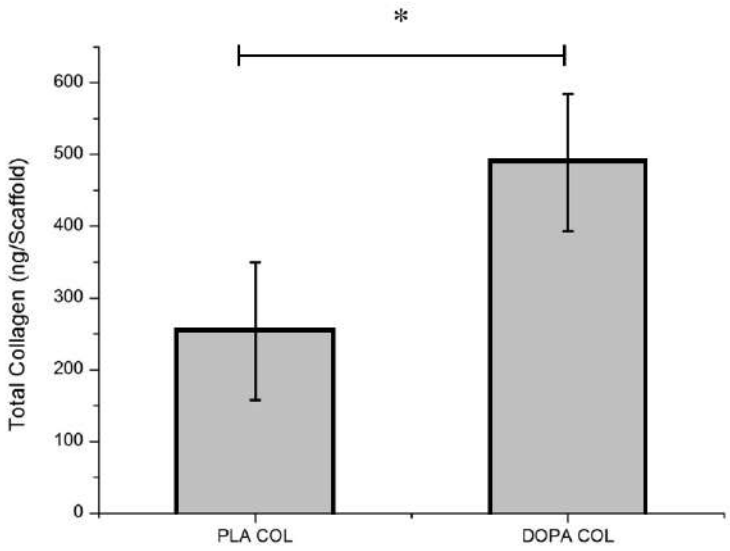

Fig.5.8. Collagen amount was measured by biochemical assay for hydroxyproline, assuming hydroxyproline-to-collagen ratio of 1: 7.69. *p<0.05

The PDA layer has the capacity to work as a bridge to covalent immobilization of proteins and biomolecules (HOU et al., 2017). Yu, Walsh and Mei (2014) (YU; WALSH; WEI, 2014) immobilized titanium surfaces with PDA and COL in order to evaluate the potential of PDA layer to improve the COL coating on to the surface. As a

result, the COL layer was better distributed and uniform in comparison with to physically bonding COL onto the surface. Other biomolecules can also be immobilized onto PDA layer. For example, bone morphogenetic protein 2 (BMP-2) was efficiently immobilized onto the surface of nanofibers of poly(l-lactic acid) (PLLA) previously coated with PDA (CHO et al., 2014). In this case, the PDA layer promoted stable BMP-2 immobilization onto the scaffold surface, improving the delivery of this molecules to cells that were cultivated onto the nanofibers and enhancing the efficiency of the material *in vivo*. However, in some cases, the stability created by the PDA layer for the covalent binding of biomolecules may reduce the concentration required to elucidate a desired regenerative effect.

5.5. Evaluation of cell response to PLA scaffolds coated with PDA and type I COL

To evaluate the cell behaviour as a response to different coatings, P700 was choose due to its intermediate properties. The cell adherence on to PLA, PLA COL, PLA DOPA and DOPA COL scaffolds, was quantified by DNA Hoechst assay after 24 hours in culture (Fig.5.9). All the groups had shown DNA amounts in the same range as the cell control samples ($5x10^5$ cells), proving that cells were efficiently seeded onto scaffold's surfaces. There was no significant difference in DNA amount between PLA and PLA COL scaffolds ($p<0.05$). However, DOPA and DOPA COL scaffolds contained a slightly higher amount of DNA in comparison with the other groups. The PDA layer has been related to the increase of cell interactions with the different materials (CHENG et al., 2016; KAO et al., 2015; TRIPATHI et al., 2016).

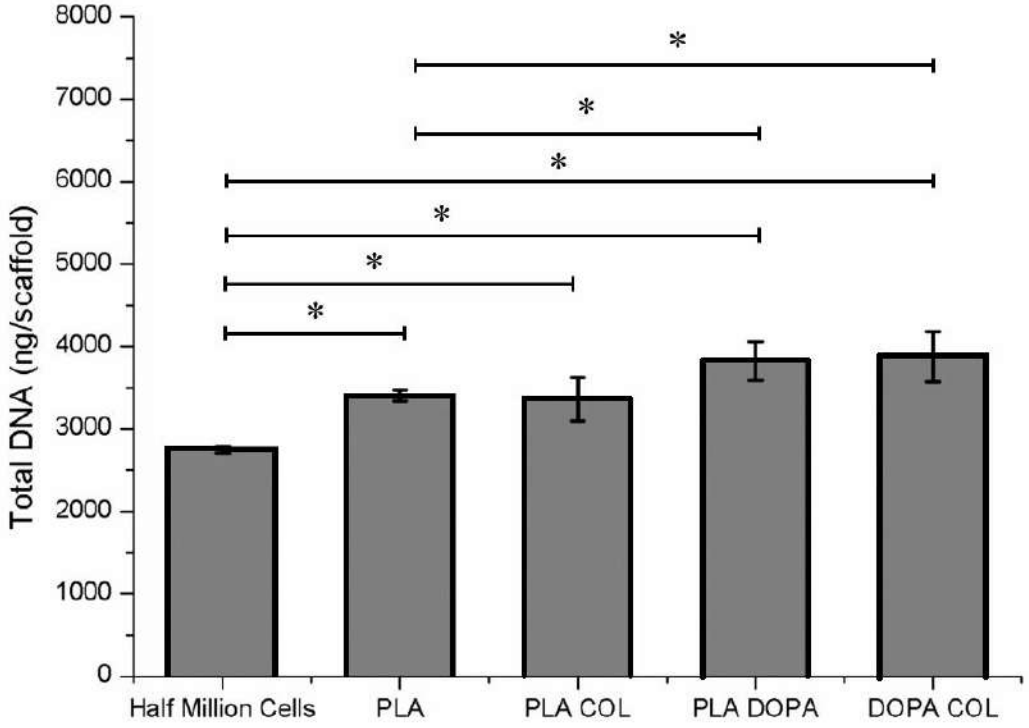

Fig.5.9. Efficiency of cell seeding on to PLA scaffolds with different coatings after 24h in culture. Cell control corresponds to $5x10^5$ cells. *$p<0.05$

The first interaction of cells with scaffold surface is important for tissue integration, whereas cell proliferation and differentiation is key to new tissue formation (CHENG et al., 2016). COL is a major protein present in ECM and contain specific sites for cell binding, enhancing the cells response. The increase in cell adhesion for PLA DOPA scaffolds (Fig.5.9) may be related to the improvement of surface hydrophilicity and the addition of functional groups (e.g., OH^-, NH_2^-) promoted by PDA coating (KU; PARK, 2010). The combination of functional groups with specific sites for cell adhesion suggests that DOPA COL scaffolds are more efficient to improve cells interactions with the surface. These results are in agreement with Hu et al. (HU et al., 2017), that produced porcine acellular dermal matrix (PADM), modified with PDA

and COL. The authors observed that cell viability and attachment was improved when PDA intermediate the COL binding onto the PADM surface.

Cell seeding onto a surface is the dissemination of isolated cells and is the first step in establishing a 3D culture and it plays a crucial role in determining the tissue growth. Static cell culture is the most common strategy to study cell response to scaffolds (MARTIN; WENDT; HEBERER, 2004). Nevertheless, cell culture under dynamic flow, in bioreactor, is a way to mimic the physiological environment, allowing a better 3D organization for cells, enhancing proliferation while maintaining their phenotype (HUTMACHER, 2000; NAVA; RAIMONDI; PIETRABISSA, 2013). The dynamic *in vitro* culture is a promising alternative to tissue engineering, since the environment is closest to that one found *in vivo*. The cell adhesion to a surface that will be cultured in bioreactor needs to be strong, since the liquid flow can leach out cells weakly adhered onto the surface. Once PDA and COL I coatings enhanced the cell adhesion in the early stage of culture, this strategy can be applied to scaffolds that will be cultured under dynamic flow, preventing cell lost.

To evaluate the MSCs viability on to PLA, PLA COL, PLA DOPA and DOPA COL scaffolds a LIVE/DEAD® assay was performed after 12 hours and 7 days of cell culture. Cells remained viable after 12 hours of culture for all scaffolds groups (Fig.5.10). After 12 hours, it was possible to observe uniform cell layer on scaffolds that were previously coated with COL (Fig.5.10 b), PDA (Fig.5.10 c) or both (Fig.5.10 d), whereas the highest amount of live cells (in green) was observed on DOPA COL scaffolds (Fig.5.10 d). After 7 days in culture, the cells remained viable (Fig.5.11) with clear evidence of robust cell proliferation. For the coated groups (Fig.5.11 b, Fig.5.11 c and Fig.5.11 d) the cells were better homogeneously distributed on the surface and,

once again, the highest amount of viable cells was observed in the group coated with PDA and COL (Fig.5.11 d).

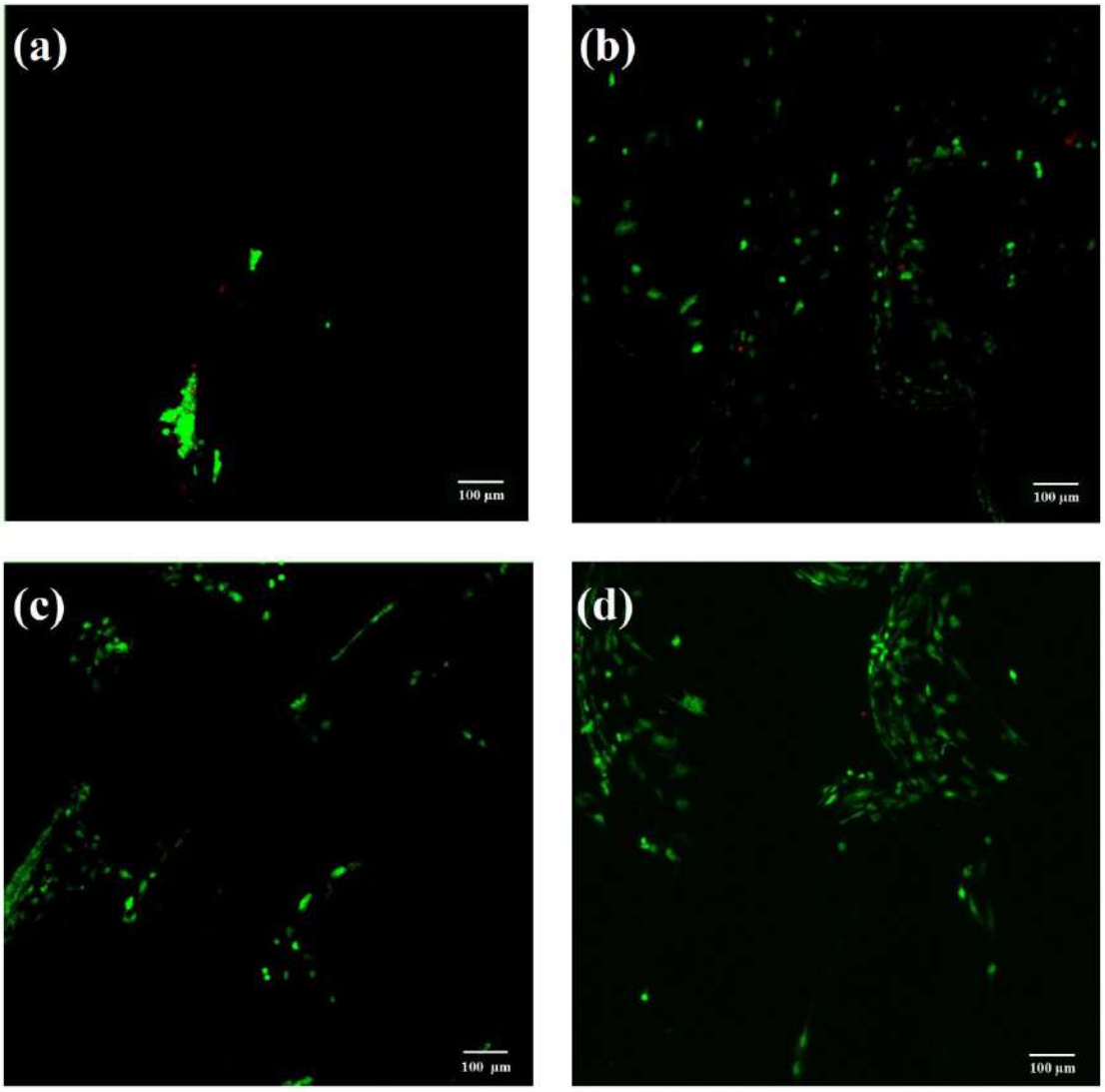

Fig.5.10. Cell viability on (a) PLA, (b) PLA COL, (c) PLA DOPA and (d) DOPA COL scaffolds. LIVE/DEAD ® assay was performed on MSCs seeded in PLA scaffolds after 12 hours of culture. Viable cells are shown in green (calcein AM) while non-viable cells are shown in red (ethidium homodimer).

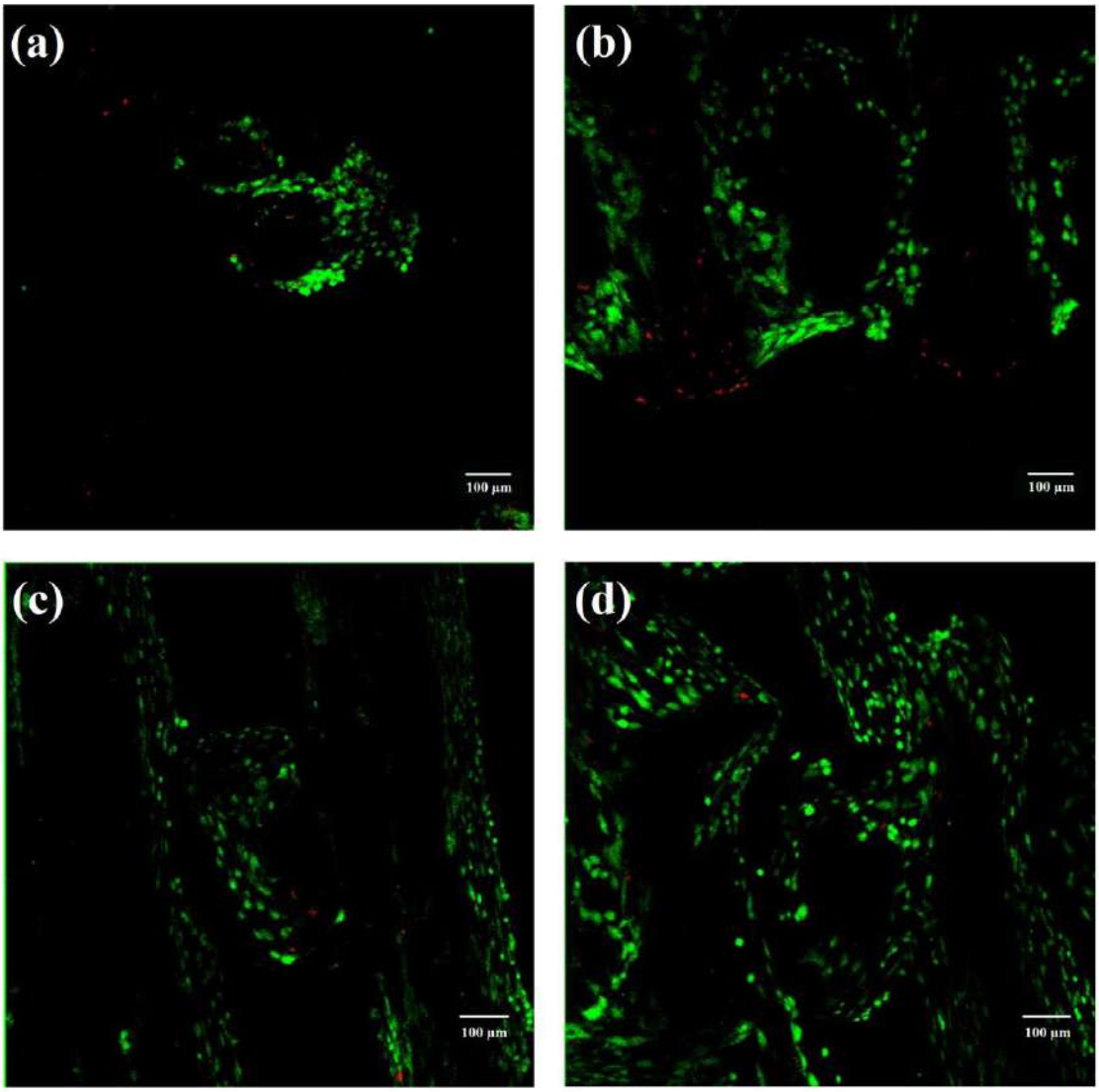

Fig.5.11. Cell viability on (a) PLA, (b) PLA COL, (c) PLA DOPA and (d) DOPA COL. Live/dead assay was performed on MSCs seeded in PLA scaffolds after 7 days of culture. Viable cells are shown in green (calcein AM) while non-viable cells are shown in red (ethidium homodimer).

Immunofluorescence for vinculin (green), actin (red) and nucleus (blue) was used to monitor cell attachment and spreading on to scaffolds surfaces. The better cell adhesion on the DOPA COL scaffolds in comparison with the other groups was confirmed and can be observed at Fig.5.12. Porcine BMSCs that were cultivated onto

PLA scaffolds for 24 hours barely adhered and spread on to the surface, adopting a round shape and forming some cell clusters (Fig.5.12 a), whereas cells seeded on to DOPA COL scaffolds exhibited normal adhesion and spreading (Fig.5.12 d). The actin was located on to the cell edge (around the cell cytoplasm) for all scaffolds groups and the vinculin seemed to be distributed around the cells cytoplasm for coated scaffold, while in PLA scaffolds the vinculin was more concentrated around cell nucleus. After 7 days, cells cultures onto DOPA COL scaffolds seems to be more aligned in comparison with cells cultured onto PLA scaffolds (Fig.5.13).

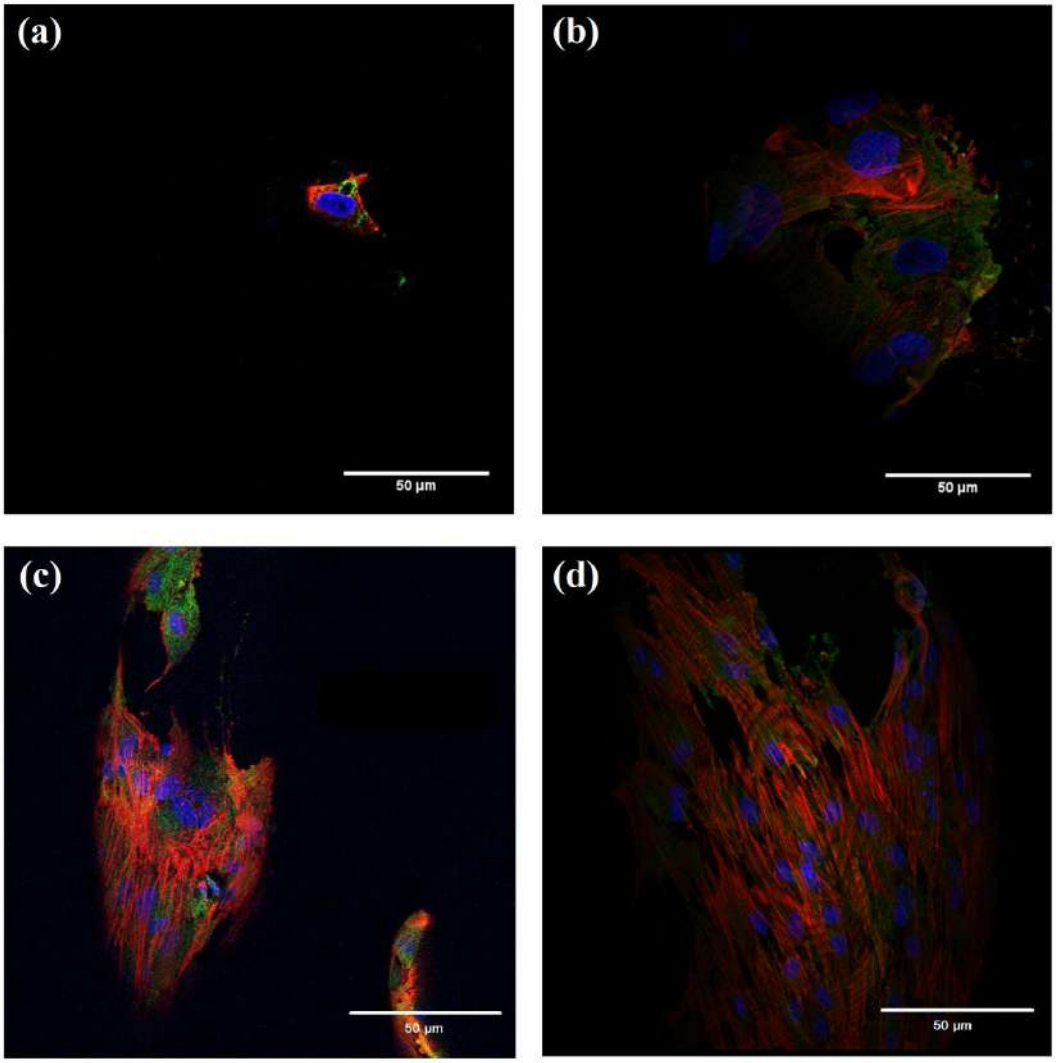

Fig.5.12. Immunofluorescense pictures of (a) PLA, (b) PLA Col, (c) PLA DOPA and (d) DOPA COL after 1 day of culture (red – actin; blue – nucleus; green – vinculin).

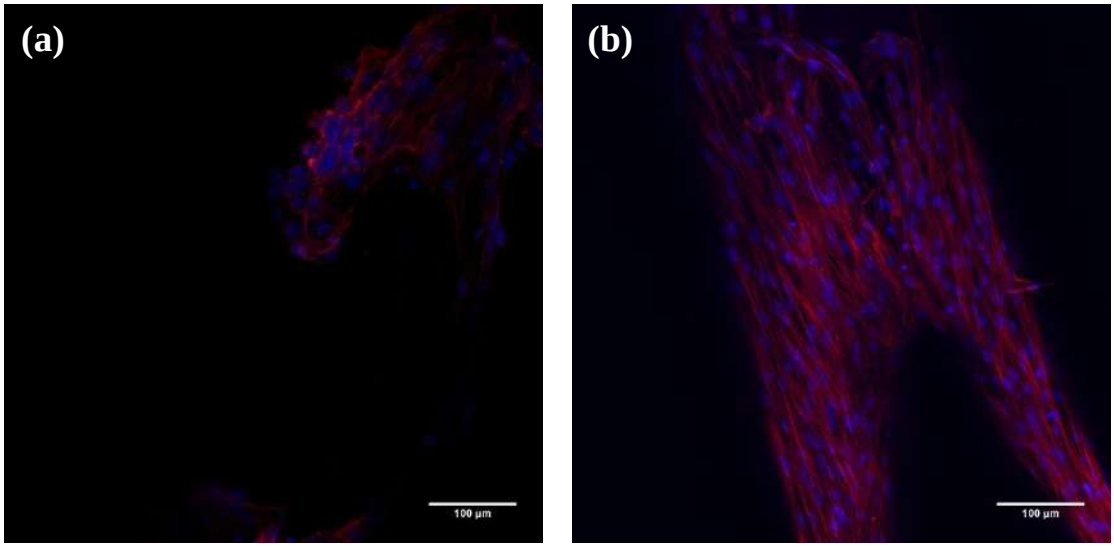

Fig.5.13. Immunofluorescence pictures of PLA (a) and DOPA COL (b) scaffolds after 7 days of culture (red – actin; blue – nucleus; green – vinculin)

The metabolic activity of the cells seeded onto PLA, PLA COL, PLA DOPA and DOPA COL scaffolds is shown in Fig.5.14. PDA layer seems to be a key factor to enhance the cell response at the beginning of cell culture. The metabolic activity of MSCs cultured onto DOPA COL was more intense over 7 days of culture in comparison with the other groups. Based on these results, the evaluation of MSCs differentiation was conducted into scaffolds with more discrepant cell behaviour: PLA and DOPA COL scaffolds. The higher metabolic activity presented by cells that were cultivated onto PLA COL, PLA DOPA and DOPA COL scaffolds may be related to the strongest adhesion onto these surfaces in comparison with PLA (Fig.5.13). Despite this, since DOPA COL scaffolds present COL specific sites and functional groups of PDA, cells that were cultivated onto this group were more active in comparison with those ones that were cultivated onto the other groups. Over time, these differences tends to decrease since cells deposit their own proteins and biomolecules onto scaffold structure.

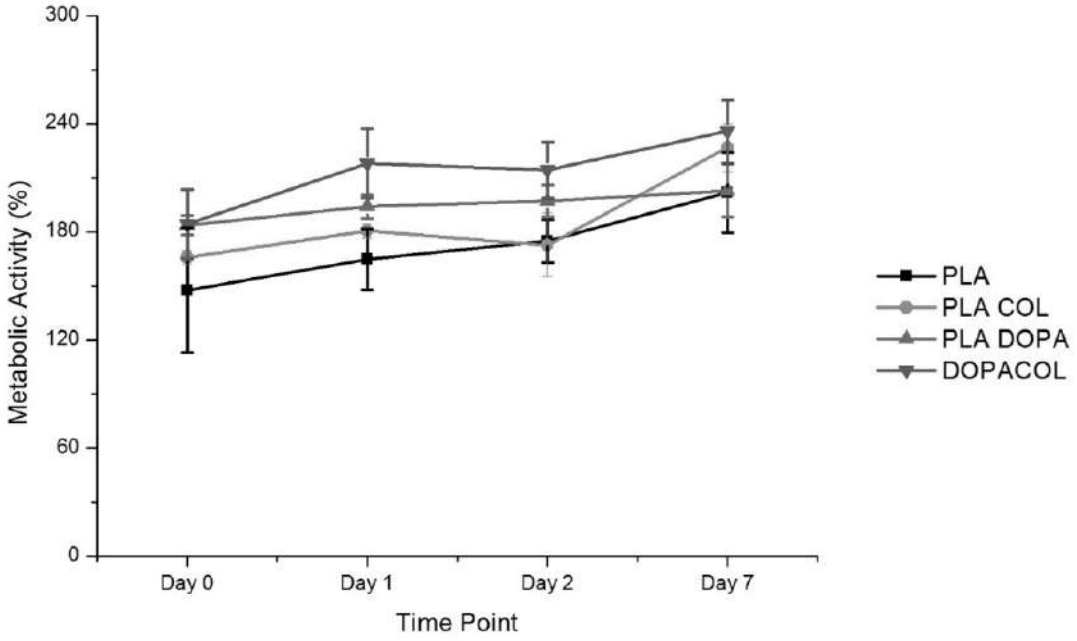

Fig.5.14. Metabolic activity of MSCs cultivated in PLA scaffolds coated, or not, with PDA and collagen. Alamar Blue assay was performed on MSCs seeded in PLA scaffolds with different coatings during 7 days.

5.5.1. Evaluation of pBMSC differentiation as a response to PDA and COL coatings

Scaffolds were seeded with MSCs and cultured for 21 days with osteogenic medium. Cells remained viable after 21 days (Fig.5.15). However, the presence of non-viable cells seems to be stronger in PLA scaffolds (Fig.5.15 a) than in DOPA COL scaffolds (Fig.5.15 b). Cell ingrowth was assessed at day 3, 7, 10 and 14 by optical microscopy, onto the surface of PLA and DOPA COL scaffolds (Fig.5.16). At day 3 (Fig.5.15 a and b) it was possible to observe ECM deposition onto the DOPA COL surface (Fig.5.16 b), whereas onto PLA (Fig.5.16 a) this deposition seems to be starting at this time. At day 3, cells seem to be infiltrating the DOPA COL scaffolds, filling in the pores. At day 7, the ECM deposition onto DOPA COL scaffolds was more apparent

than onto PLA scaffolds, with a robust layer of ECM present coating the DOPA COL fillament. In Fig.5.16 d was possible to see an intense ECM deposition onto DOPA COL surface, with a circular opening in the middle of pore space. Starting at day 14 (Fig.5.16 g and h) ECM deposition seems to be similar to that of PLA and DOPA COL scaffolds. A significant portion of the pore volume is occupied by ECM for both groups.

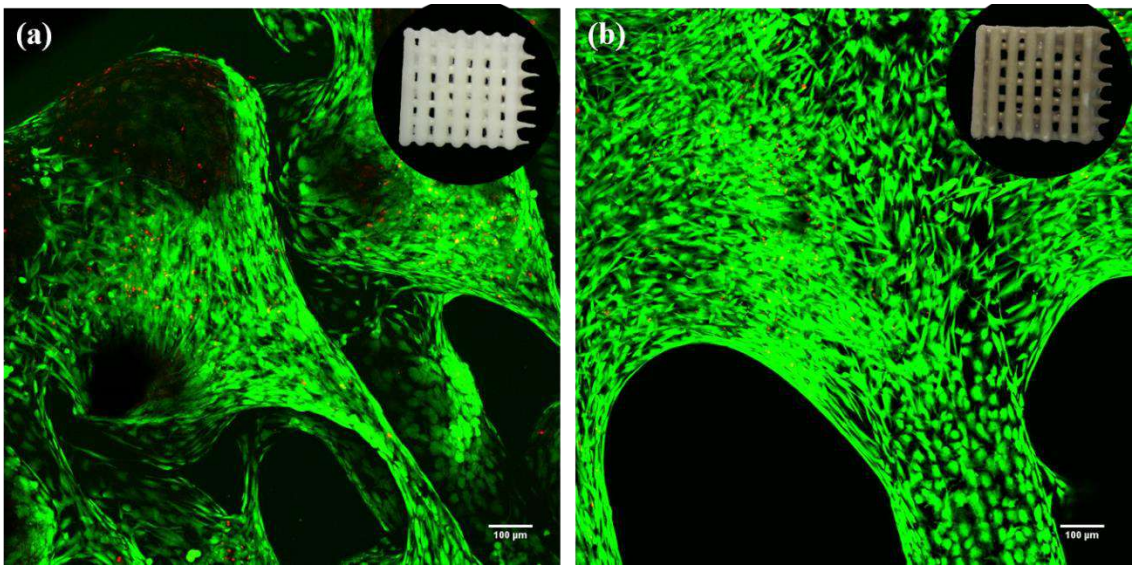

Fig.5.15. Cell viability on (a) PLA and (b) DOPA COL scaffolds. Live/dead assay was performed on MSCs seeded in PLA and DOPA COL scaffolds after 21 day of culture. Live cells are shown in green (calcein AM) while dead cells are shown in red (ethidium homodimer).

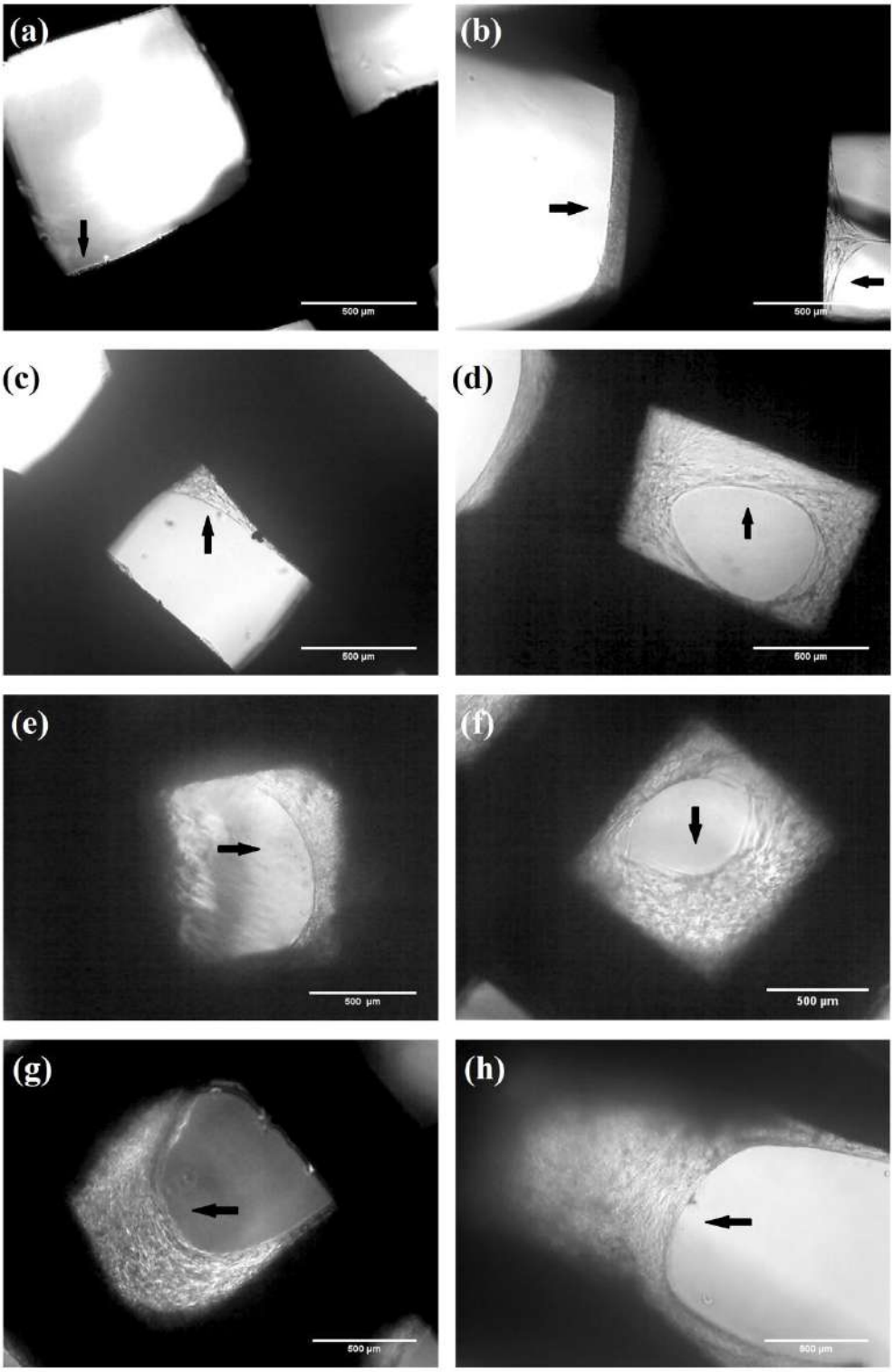

Fig. 5.16. Cell ingrowth on PLA (a, c, e, g) and DOPA COL (b, d, f, h) scaffolds. Representative phase contrast images of cell-seeded scaffolds at 10× magnification after 3 (a, b), 7 (c, d), 10 (e, f) and 14 days of culture (g, h) (n = 5). Arrows indicate cell growth and neo-tissue deposition.

BMSCs proliferated onto PLA and DOPA COL scaffolds during the 21 days of culture (Fig.5.17). At days 14 and 21 there is no significant difference in the DNA amount on PLA and DOPA COL scaffolds (Fig.5.17 a). Cells start to produce and deposit ECM in the first stages of cell culture. By day 14 there is a strong presence of ECM onto PLA scaffolds which is likely dominating the cell response at these later time. In the earlier stages of cell culture, there is a significant difference for DNA amount, metabolic activity and cell morphology between PLA and DOPA COL scaffolds. Over time, these differences tends to decrease since the deposition of proteins and biomolecules from cells over the scaffolds might create a coating, changing the surface and making the environment more attractive for cell survival and tissue growth.

Bone ECM consists, mainly, of collagen fibres (10–30%), inorganic mineral phase, that appear as small crystals (60-70%) and water (10-20%) (WANG et al., 2015b). A biochemical assay was conducted to evaluate the deposition of COL and calcium by the cells cultivated onto PLA and DOPA COL surfaces (Fig.5.17 b and c) over 21 days. At day 14, there is an accentuated difference in the COL deposition by the cells seeded onto DOPA COL scaffolds in comparison with those ones seeded onto PLA scaffolds (Fig.5.17 b). On the coated surface, the total COL deposited was 98% higher than on PLA scaffolds. At day 21 there is no significant difference for COL deposition between the groups. For calcium deposition, at day 14 a slight increase of 30% occurs for DOPA COL scaffolds in comparison with PLA. As day 21, no significant difference was observed between the groups (Fig.5.17 c). These observations corroborate the hypothesis presented in last paragraph in which, in long-term culture, the environmental is changed by cells since they deposit their own ECM proteins.

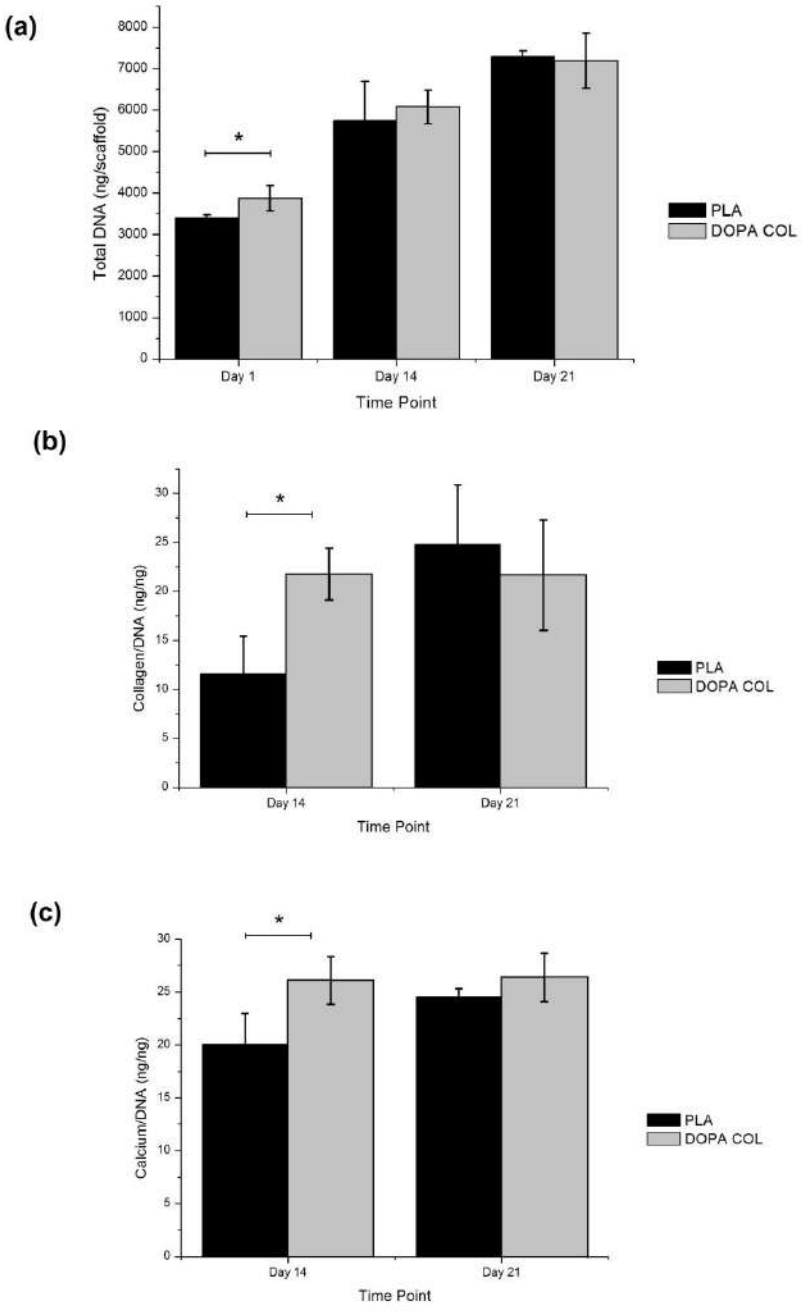

Fig.5.17. Biochemical analyses for (a) total amount of DNA at Day 1, Day 14 and Day 21, (b) Collagen/DNA rate at Day 14 and 21 and (c) Calcium/DNA rate at Day 14 and 21 estimated by amount of Hydroxyproline. *$p<0.05$

ALP, an early osteogenic protein marker (MAO; SHIN; MOONEY, 2016), was quantified by biochemical assay (Fig.5.18), in order to evaluate how the coating is

affecting the cells differentiation. Porcine BMSCs seeded onto DOPA COL scaffolds and cultured in Low Glucose medium produced more than 500% of ALP in comparison with those one cultured onto PLA scaffolds in the same medium.

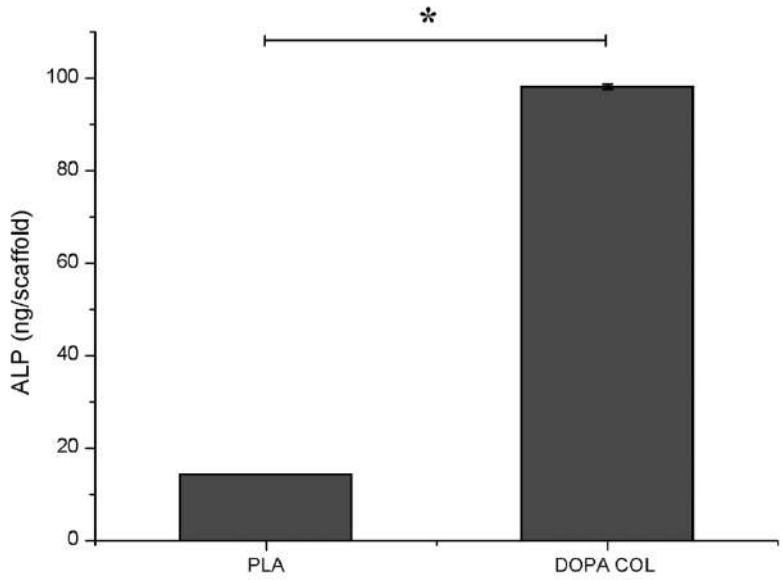

Fig.5.18. ALP content measured in the supernadant of PLA and DOPA COL scaffolds, cultured with MSCs for 21 days. *p<0.05

Several studies point to PDA coating as a tool to enhance the osteogenesis process in different surfaces (CHENG et al., 2016; KAO et al., 2015; YU et al., 2017). The expressive increase in ALP produced by cells that were cultivated onto DOPA COL scaffolds indicate that the PDA and COL coating can stimulate the early stages of osteogenic differentiation and can act as a key to stimulate the bone tissue regeneration (RIM et al., 2012; YEH et al., 2015).

Scaffolds that were coated with PDA and COL I presented the best condition to stimulate cell adhesion, ECM deposition and ALP activity. To evaluate the influence of

strut spacing in cell response, the study was conducted with DOPA COL scaffolds with different geometries.

5.6. Influence of pore size in cell behaviour

A 3D matrix for tissue engineering will act as a temporary matrix to support cell growth and the deposition of Extracellular Matrix (ECM) (ATALA, 2007). Therefore, scaffolds that are employed to regenerate a load-bearing tissue (bone, cartilage) need to endure the load that is usually imposed *in situ* (STEVENS, 2008).

Cell adhesion and growth were assessed at day 14 and day 21 of cell culture. Cells appear attached to the scaffolds surface during the whole culture period. After 14 days it was possible to observe a thick cell layer within all scaffolds (Fig.5.19), indicating robust cell proliferation and ECM deposition. It was possible to observe a partial filling of pores in scaffolds P500. After 21 days, pores of P500 scaffolds appeared to be completed filled with cells and ECM. These differences are explained by the variation of strut spacing, which create a difference in the pore size (Table 5.1). The smaller pores of P500 scaffolds were filled faster than large pores in the other scaffolds which require more time and more extracellular matrix deposition to occupy the whole pore space.

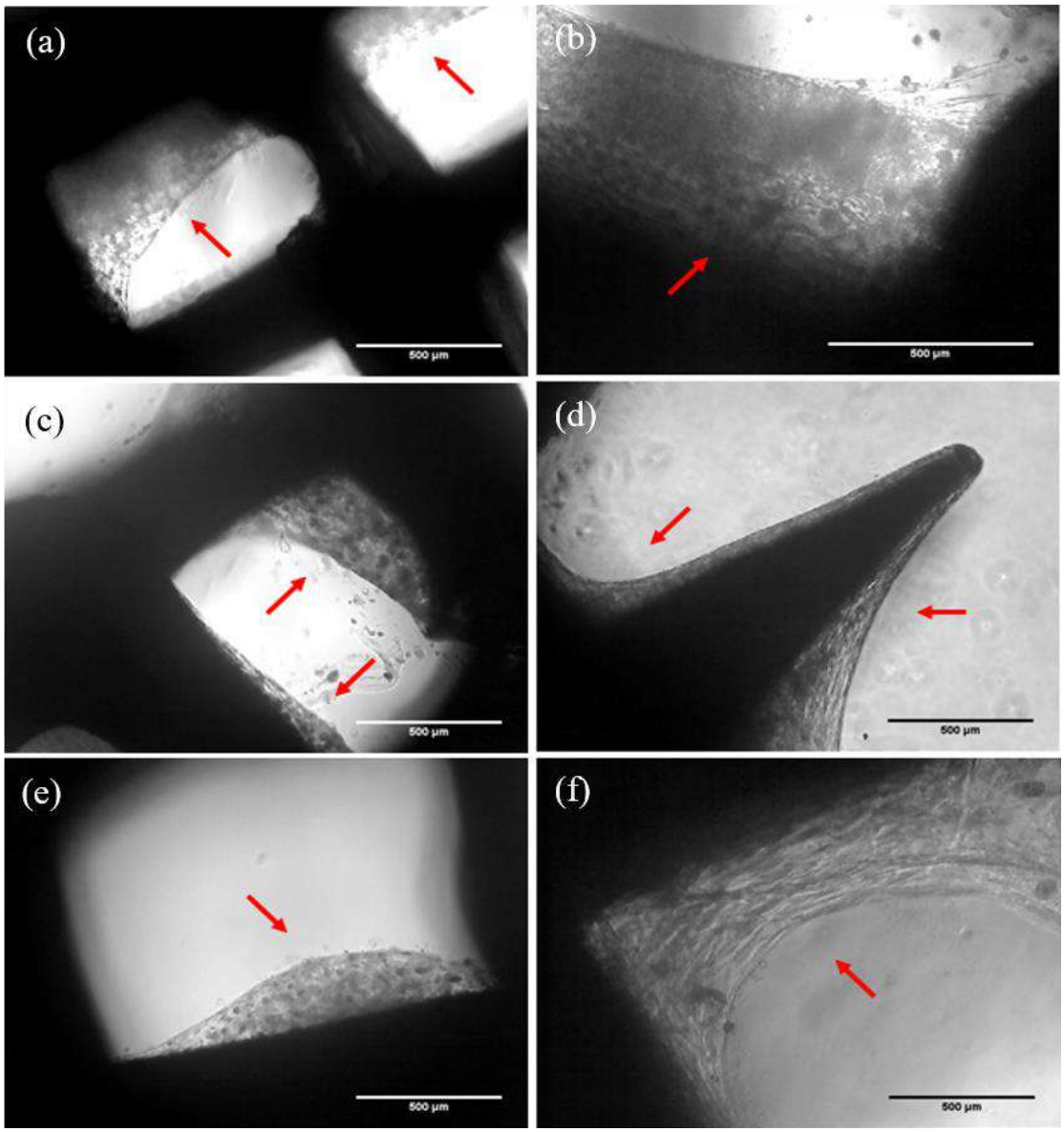

Fig.5.19. MSCs ingrowth onto PLA scaffolds P500 (a,b),P700 (c, d) and P900 (e, f) after 14 (a, c and e) and 21 days (b, d and f). Red arrows indicate the cell layer on the black (non-transparent) scaffolds and the scale bar denotes 500 µm.

After 21 days of culture, the total DNA content was higher than at the first day in culture, indicating intense cell proliferation for all groups (Fig.5.20 a). Calcium and collagen deposition was measured by biochemical assay. Cells deposited calcium and

collagen within all scaffold groups, without significant difference between them (Fig.5.20 b and 6c, respectively). The difference in porosity seems not affect the rate of ECM deposition during the 21 days of culture. Despite this, since P500 tend to be filled faster than the other groups, cells cultured in this group may be impaired by the lack of nutrients and oxygen availability if maintained in long-term culture. Therefore, larger pores scaffolds may better support *in vitro* cell culture for longer periods. Although there is no significant difference in the deposition of ECM for cells cultures in PLA scaffolds with different strut spacing, some studies show that cells can secret more ECM compounds when cultured in large space. In contrast, cells grow faster when cultured in scaffolds with smaller pore space, secreting less ECM compounds (ANNABI et al., 2010; LIEN; KO; HUANG, 2009; OSTROWSKA et al., 2016)

The ideal pore size varies according the target tissue. As an example, Zhang et al. (2014) evaluated the effect of pore size on cartilage regeneration. The authors produced collagen scaffolds with four different pore sizes from ice particulates with diameter of 150–250, 250–355, 355–425 and 425–500 μm. They did not observe significant influence of pore size in chondrocites proliferation *in vitro* and *in vivo*, nonetheless it was possible to observe the influence of pore size on cartilage regeneration *in vivo*. Scaffolds that were prouced from particulates with 150-250 μm in size showed higher expression and production of type II COL and aggrecan, increasing the formation of cartilage with mechanical stability (ZHANG et al., 2014). On the other hand, Zhao et al. (2016) investigated the effect of pore size and surface chemistry of 3D porous scaffolds regulate the fate of MSCs *in vitro* in combination. 3D porous PCL scaffolds with varying pore sizes (100–200 μm, 200–300 μm and 300–450 μm) were fabricated and subjected to either hydrolysis or aminolysis. Pore size in the range of 200–300 μm with hydrolysis in 3D scaffolds was the most favorable condition for

growth of hMSCs. Pores in the range of 200–300 μm with hydrolysis for 1 h supported the best osteogenic differentiation of hMSCs while the chondrogenic differentiation was greatest in scaffolds with a pore size of 300–450 μm and treated with aminolysis for 1 h. These studies bring to light not only that different cell lineage presents differents behaviors for scaffolds with different pore sizes but also that pore size tend to affect architecture and functionality of restores tissue.

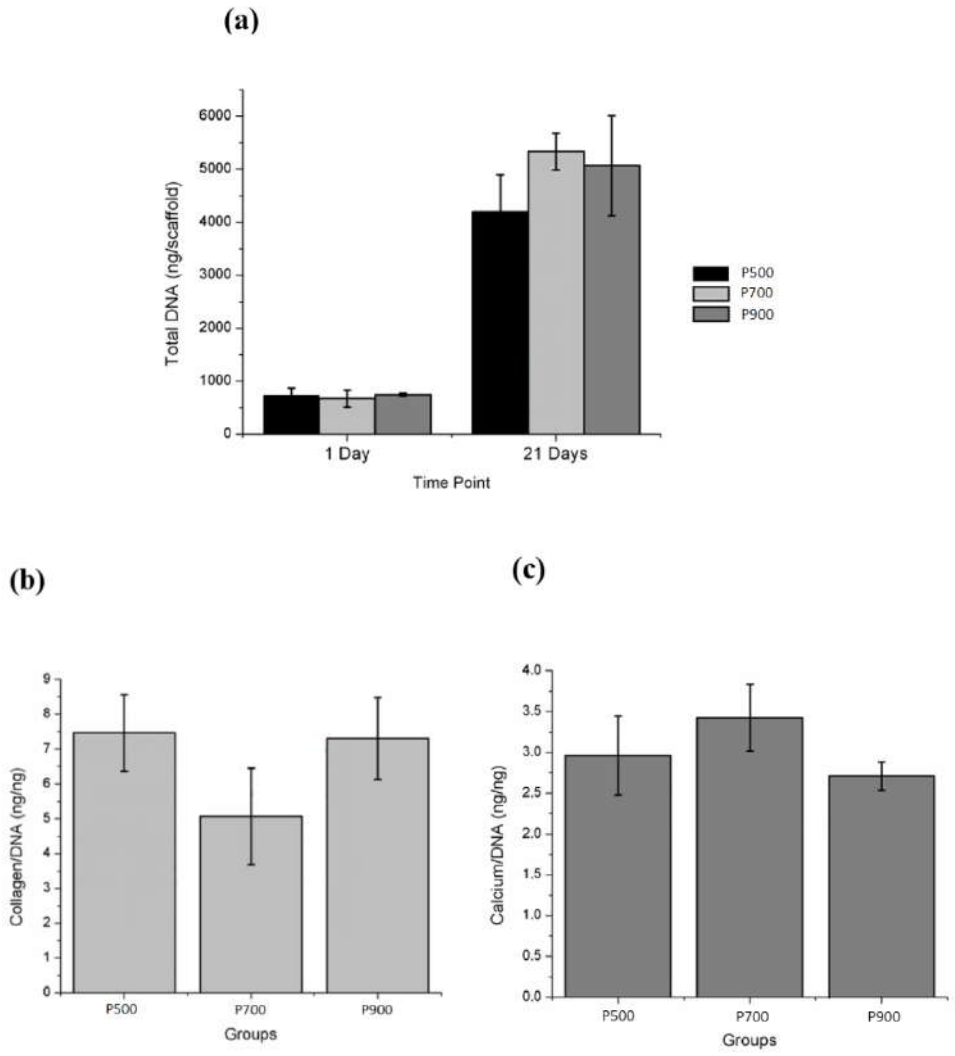

Fig.5.19. Biochemical analysis of PLA scaffolds at day 21 of in vitro culture: (a) Total DNA, (b) collagen and (c) calcium accumulation within constructs. Significance: *P < 0.05. Three or four constructs were analysed biochemically at each time point.

6. Conclusion

Fused deposition modelling was successfully applied to produce PLA scaffolds with highly interconnected pores. Despite the variation in strut spacing affecting the porosity and mechanical properties, all groups presented maximum stress and Elastic point in the same range as cancellous bone. The printing method allows producing parts with high accuracy in comparison with the virtual model and high reproducibility. PDA and COL were successfully immobilized onto PLA surface and, as expected, the PDA layer helps to increase the amount of COL on the surface.

The PDA plus COL I layer also affect the deposition of ECM compounds up to 14 days and after this period there is no significant difference with uncoated PLA. However, PDA plus COL I coating raise substantially the production of alkaline phosphatase (ALP), an osteogenic marker. Cells were growing and filling in the pore space of all the groups. Although there is no significant difference in cell number and ECM deposition among scaffolds with different porosities, pore lumen of P500 was filled in faster than pore lumen of P500 and P900. it is possible to assume that the parameters can be modified for clinical applications according to the mechanical load of the implanted site. In other words, the strut spacing can be adapted according the physiological and anatomical characteristic of the bone tissue that need to be repaired.

The PLA scaffolds manufactured in this work can be applied as a material to enhance bone tissue regeneration. It can be suggested that 3D-printed polymeric scaffolds with tetragonal pores with 700 µm in size provide appropriate porosity and mechanical properties for bone tissue ingrowth, enabling adequate nutrient and oxygen transport to cells resident within the center of the scaffolds. Moreover, the method for surface modification by direct immersion of constructs into the PDA and COL I

solutions seems to be a useful and efficient approach to enhance biomolecule adhesion across numerous different TE platforms.

7. Suggestions to future works

As suggestions to future experiments, in order to enhance the results that were obtained in this work, the following steps are proposed:

- To evaluate the expression of osteogenic markers by molecular biology, in order to attest the PDA potential to induce osteogenesis;
- To evaluate the potential of PDA coating to induce vascularization under different cell culture conditions;
- To analyze the cell response in dynamical in *vitro study;*
- To evaluate the *in vivo* response to cell-free and cell cultured PLA scaffolds coated with PDA and COL;
- To characterize PLA scaffolds coated with PDA after long term culture;
- To evaluate the potential of FBS proteins to adhere in PLA scaffolds coated with PDA.

8. References

ALLAF, R. M. et al. Porous poly(e-caprolactone) scaffolds for load-bearing tissue regeneration: Solventless fabrication and characterization. **Journal of Biomedical Materials Research - Part B Applied Biomaterials**, v. 101 B, n. 6, p. 1050–1060, 2013.

ALMEIDA, C. R. et al. Impact of 3-D printed PLA- and chitosan-based scaffolds on human monocyte/macrophage responses: Unraveling the effect of 3-D structures on inflammation. **Acta Biomaterialia**, v. 10, n. 2, p. 613–622, 2014.

ANNABI, N. et al. Controlling the Porosity and Microarchitecture of Hydrogels for Tissue Engineering. **Tissue Engineering Part B: Reviews**, v. 16, n. 4, p. 371–383, 2010.

ATALA, A. Engineering tissues, organs and cells. **Journal of Tissue Engineering and Regenerative Medicine**, v. 1, n. 2, p. 83–96, mar. 2007.

ATALA, A. Regenerative medicine strategies. **Journal of Pediatric Surgery**, v. 47, n. 1, 2012.

BOSCHETTO, A.; BOTTINI, L. Accuracy prediction in fused deposition modeling. **International Journal of Advanced Manufacturing Technology**, v. 73, n. 5–8, p. 913–928, 2014.

CARLOS, A. L. M.; MAIA-PINTO, M. DE O. C.; THIRÉ, R. M. DA S. M. Caracterização Morfológica de arcabouços de PLA/cHA produzidos por tecnologia de impressão 3D. **9º Congresso Latino-Americano de Orgãos Artificiais e Biomateriais 13º Congresso da Sociedade Latino Americana de Biomateriais, Orgãos Artificiais e Engenharia de Tecidos - SLABO.** 2016 Disponível em: <http://www.metallum.com.br/9colaob/anais/PDF/12-005TT.pdf>

CARRASCO, F. et al. Processing of poly(lactic acid): Characterization of chemical structure, thermal stability and mechanical properties. **Polymer Degradation and Stability**, v. 95, n. 2, p. 116–125, 2010.

CERETTI, E. et al. Multi-layered Scaffolds Production via Fused Deposition Modeling (FDM) Using an Open Source 3D Printer: Process Parameters Optimization for Dimensional Accuracy and Design Reproducibility. **Procedia CIRP**, v. 65, p. 13–18, 2017.

CHEN, F. M.; LIU, X. Advancing biomaterials of human origin for tissue engineering. **Progress in Polymer Science**, v. 53, p. 86–168, 2016.

CHENG, Y.-L. et al. Enhanced adhesion and differentiation of human mesenchymal stem cell inside apatite-mineralized/poly(dopamine)-coated poly(?-caprolactone) scaffolds by stereolithography. **Journal of Materials Chemistry B**, v. 4, n. 38, p. 6307–6315, 2016.

CHENG, Z.; TEOH, S. H. Surface modification of ultra thin poly (??-caprolactone) films using acrylic acid and collagen. **Biomaterials**, v. 25, n. 11, p. 1991–2001, 2004.

CHIA, H. N.; WU, B. M. Recent advances in 3D printing of biomaterials. **Journal of Biological Engineering**, v. 9, n. 1, p. 4, 2015.

CHO, H. et al. Effective Immobilization of BMP ‐ 2 Mediated by Polydopamine Coating on Biodegradable Nano fi bers for Enhanced in Vivo Bone Formation. **Applied Materials & Intarfaces**, v. 6, p. 11225–11235, 2014.

DING, Y. H.; FLOREN, M.; TAN, W. Mussel-inspired polydopamine for bio-surface functionalization. **Biosurface and Biotribology**, v. 2, n. 4, p. 121–136, 2016.

DOMINGOS, M. et al. Improved osteoblast cell affinity on plasma-modified 3-D extruded PCL scaffolds. **Acta Biomaterialia**, v. 9, n. 4, p. 5997–6005, 2013.

FERNANDEZ-YAGUE, M. A. et al. Biomimetic approaches in bone tissue engineering: Integrating biological and physicomechanical strategies. **Advanced Drug Delivery Reviews**, v. 84, p. 1–29, abr. 2015.

FLORENCIO-SILVA, R. et al. Biology of Bone Tissue: Structure, Function, and Factors That Influence Bone Cells. **BioMed Research International**, v. 2015, p. 1–17, 2015.

GIBSON, L. J. Biomechanics of cellular solids. **Journal of Biomechanics**, v. 38, n. 3, p. 377–399, 2005.

GODDARD, J. M.; HOTCHKISS, J. H. Polymer surface modification for the attachment of bioactive compounds. **Progress in Polymer Science (Oxford)**, v. 32, n. 7, p. 698–725, 2007.

HABIB, F. N. et al. Design and Development of Scaffolds for Tissue Engineering Using Three-Dimensional Printing for Bio-Based Applications. **3D Printing and Additive Manufacturing**, v. 3, n. 2, p. 119–127, 2016.

HADDAD, T. et al. Fabrication and surface modification of poly lactic acid (PLA) scaffolds with epidermal growth factor for neural tissue engineering. **Biomatt**, v. 6, n. 1, p. 1–12, 2016.

HAMAD, K. et al. Properties and medical applications of polylactic acid: A review. **Express Polymer Letters**, v. 9, n. 5, p. 435–455, 2015.

HOU, J. et al. Guided protein/cell patterning on superhydrophilic polymer brushes functionalized with mussel-inspired polydopamine coatings. **ChemComm**, v. 53, p. 6708–6711, 2017.

HU, Y. et al. Development of collagen/polydopamine complexed matrix as mechanically enhanced and highly biocompatible semi-natural tissue engineering scaffold. **Acta Biomaterialia**, v. 47, p. 135–148, jan. 2017.

HUTMACHER, D. W. **Scaffolds in tissue engineering bone and cartilage**. [s.l.] Woodhead Publishing Limited, 2000. v. 21

HUTMACHER, D. W. et al. State of the art and future directions of scaffold-based bone engineering from a biomaterials perspective. **Journal of Tissue Engineering and Regenerative Medicine**, v. 1, n. 4, p. 245–260, jul. 2007.

HUTMACHER, D. W.; SITTINGER, M.; RISBUD, M. V. Scaffold-based tissue engineering: Rationale for computer-aided design and solid free-form fabrication systems. **Trends in Biotechnology**, v. 22, n. 7, p. 354–362, 2004.

IKADA, Y. Surface modification of polymers for medical applications. **Biomaterials**, v. 15, n. 10, p. 725–736, 1994.

JAFARI, M. et al. Polymeric scaffolds in tissue engineering: a literature review. **Journal of Biomedical Materials Research Part B: Applied Biomaterials**, v. 105, n.

2, p. 431–459, fev. 2015.

KALITA, S. J. et al. Development of controlled porosity polymer-ceramic composite scaffolds via fused deposition modeling. **Materials Science and Engineering C**, v. 23, n. 5, p. 611–620, 2003.

KANCZLER, J. Osteogenesis and angiogenesis : the potential for engineering bone. **European Cells and Materials**, v. 15, p. 100–114, 2008.

KAO, C. et al. Poly (dopamine) coating of 3D printed poly (lactic acid) scaffolds for bone tissue engineering. **Materials Science and Engineering C**, v. 56, p. 165–173, 2015.

KARAGEORGIOU, V.; KAPLAN, D. Porosity of 3D biomaterial scaffolds and osteogenesis. **Biomaterials**, v. 26, n. 27, p. 5474–5491, 2005.

KIM, H. W. et al. Oxygen concentration control of dopamine-induced high uniformity surface coating chemistry. **ACS Applied Materials and Interfaces**, v. 5, n. 2, p. 233–238, 2013.

KIM, T. G.; SHIN, H.; LIM, D. W. Biomimetic scaffolds for tissue engineering. **Advanced Functional Materials**, v. 22, n. 12, p. 2446–2468, 2012.

KORPELA, J. et al. Biodegradable and bioactive porous scaffold structures prepared using fused deposition modeling. **Journal of Biomedical Materials Research - Part B Applied Biomaterials**, v. 101, n. 4, p. 610–619, 2013.

KU, S. H. et al. General functionalization route for cell adhesion on non-wetting surfaces. **Biomaterials**, v. 31, n. 9, p. 2535–2541, 2010.

KU, S. H.; LEE, J. S.; PARK, C. B. Spatial control of cell adhesion and patterning through mussel-inspired surface modification by polydopamine. **Langmuir**, v. 26, n. 19, p. 15104–15108, 2010.

KU, S. H.; PARK, C. B. Human endothelial cell growth on mussel-inspired nanofiber scaffold for vascular tissue engineering. **Biomaterials**, v. 31, n. 36, p. 9431–9437, 2010.

LASPRILLA, A. J. R. et al. Poly-lactic acid synthesis for application in biomedical devices - A review. **Biotechnology Advances**, v. 30, n. 1, p. 321–328, 2012.

LEE, H. et al. Mussel-Inspired Surface Chemistry for Multifunctional Coatings. **Science**, v. 318, n. 5849, p. 426–430, 2007.

LEE, J. S. et al. Effect of pore architecture and stacking direction on mechanical properties of solid freeform fabrication-based scaffold for bone tissue engineering. **Journal of Biomedical Materials Research - Part A**, v. 100 A, n. 7, p. 1846–1853, 2012.

LEONG, K. F.; CHEAH, C. M.; CHUA, C. K. Solid freeform fabrication of three-dimensional scaffolds for engineering replacement tissues and organs. **Biomaterials**, v. 24, n. 13, p. 2363–2378, 2003.

LIEN, S. M.; KO, L. Y.; HUANG, T. J. Effect of pore size on ECM secretion and cell growth in gelatin scaffold for articular cartilage tissue engineering. **Acta Biomaterialia**, v. 5, n. 2, p. 670–679, 2009.

LOH, Q. L.; CHOONG, C. Three-Dimensional Scaffolds for Tissue Engineering Applications: Role of Porosity and Pore Size. **Tissue Engineering Part B: Reviews**, v. 19, n. 6, p. 485–502, dez. 2013.

MADHURAKKAT PERIKAMANA, S. K. et al. Materials from Mussel-Inspired Chemistry for Cell and Tissue Engineering Applications. **Biomacromolecules**, v. 16, n. 9, p. 2541–2555, 2015.

MAO, A. S.; SHIN, J. W.; MOONEY, D. J. Effects of substrate stiffness and cell-cell contact on mesenchymal stem cell differentiation. **Biomaterials**, v. 98, p. 184–191, 2016.

MARTIN, I.; WENDT, D.; HEBERER, M. The role of bioreactors in tissue engineering. **Trends in Biotechnology**, v. 22, n. 2, p. 80–86, 2004.

MOHAMED, O. A.; MASOOD, S. H.; BHOWMIK, J. L. Optimization of fused deposition modeling process parameters: a review of current research and future prospects. **Advances in Manufacturing**, v. 3, n. 1, p. 42–53, 2015.

MURPHY, C. M. et al. Effect of collagen-glycosaminoglycan scaffold pore size on matrix mineralization and cellular behavior in different cell types. **Journal of Biomedical Materials Research - Part A**, v. 104, n. 1, p. 291–304, 2016.

MURPHY, C. M.; HAUGH, M. G.; O'BRIEN, F. J. The effect of mean pore size on cell attachment, proliferation and migration in collagen-glycosaminoglycan scaffolds for bone tissue engineering. **Biomaterials**, v. 31, n. 3, p. 461–466, 2010.

NADERI, H.; MATIN, M. M.; BAHRAMI, A. R. Review paper: Critical Issues in Tissue Engineering: Biomaterials, Cell Sources, Angiogenesis, and Drug Delivery Systems. **Journal of Biomaterials Applications**, v. 26, n. 4, p. 383–417, 2011.

NAVA, M. M.; RAIMONDI, M. T.; PIETRABISSA, R. A multiphysics 3D model of tissue growth under interstitial perfusion in a tissue-engineering bioreactor. **Biomechanics and Modeling in Mechanobiology**, v. 12, n. 6, p. 1169–1179, 2013.

NEREM, R. M.; SAMBANIS, A. Tissue Engineering: From Biology to Biological Substitutes. **Tissue Engineering**, v. 1, n. 1, p. 3–13, 1995.

O'BRIEN, C. et al. 3D Printing of Nanomaterial Scaffolds for Complex Tissue Regeneration. **Tissue Engineering Part B: Reviews**, v. 21, n. 1, p. 1–45, 2015.

O'BRIEN, F. J. Biomaterials & scaffolds for tissue engineering. **Materials Today**, v. 14, n. 3, p. 88–95, 2011.

OKANO, T. Current Progress of Cell Sheet Tissue Engineering and Future Perspective. **Tissue Engineering Part A**, v. 20, n. 9–10, p. 1353–1354, maio 2014.

OLIVEIRA, M. F. et al. Construção de Scaffolds para engenharia tecidual utilizando prototipagem rápida. **Matéria (Rio de Janeiro)**, p. 373–382, 2007.

OSTROWSKA, B. et al. Influence of internal pore architecture on biological and mechanical properties of three-dimensional fiber deposited scaffolds for bone regeneration. **Journal of Biomedical Materials Research - Part A**, v. 104, n. 4, p. 991–1001, 2016.

RASAL, R. M.; HIRT, D. E. Poly(lactic acid) toughening with a better balance of properties. **Macromolecular Materials and Engineering**, v. 295, n. 3, p. 204–209, 2010.

RIM, N. G. et al. Mussel-inspired surface modification of poly(l-lactide) electrospun fibers for modulation of osteogenic differentiation of human mesenchymal stem cells. **Colloids and Surfaces B: Biointerfaces**, v. 91, n. 1, p. 189–197, 2012.

ROACH, P. et al. Modern biomaterials: A review - Bulk properties and implications of surface modifications. **Journal of Materials Science: Materials in Medicine**, v. 18, n. 7, p. 1263–1277, 2007.

ROSENZWEIG, D. H. et al. 3D-printed ABS and PLA scaffolds for cartilage and nucleus pulposustissue regeneration. **International Journal of Molecular Sciences**, v. 16, n. 7, p. 15118–15135, 2015.

SANTORO, M. et al. Poly(lactic acid) nanofibrous scaffolds for tissue engineering. **Advanced Drug Delivery Reviews**, v. 107, p. 206–212, 2016.

SEARS, N. A. et al. A Review of Three-Dimensional Printing in Tissue Engineering. **Tissue Engineering Part B: Reviews**, v. 22, n. 4, p. 298–310, ago. 2016.

SERRA, T. et al. 3D printed PLA-based scaffolds. **Organogenesis**, v. 9, n. 4, p. 239–244, 2013.

SHAFIEE, A.; ATALA, A. Tissue Engineering: Toward a New Era of Medicine. **Annual Review of Medicine**, v. 68, n. 1, p. 29–40, 2017.

SHRIVATS, A. R.; MCDERMOTT, M. C.; HOLLINGER, J. O. Bone tissue engineering : state of the union. **Drug Discovery Today**, v. 19, n. 6, p. 781–786, 2014.

SOUNESS, A. et al. Influence of scaffold design on 3D printed cell constructs. **Journal of Biomedical Materials Reasearch Part B**, p. 1–13, 2017.

SOUSA, I. et al. Collagen surface modified poly(ε-caprolactone) scaffolds with improved hydrophilicity and cell adhesion properties. **Materials Letters**, v. 134, p. 263–267, 2014.

STEEVES, A. J. et al. Evaluation of the direct effects of poly(dopamine) on the in vitro response of human osteoblastic cells. **Journal of Materials Chemistry B**, v. 4, n. 18, p. 3145–3156, 2016.

STEVENS, M. M. Biomaterials for bone tissue engineering. **Materials Today**, v. 11, n. 5, p. 18–25, 2008.

SUSMITA BOSE, M. R.; BANDYOPADHYAY, A. Recent advances in bone tissue engineering scaffolds. **Trends Biotechnology**, v. 30, n. 10, p. 546–554, 2012.

TANIGUCHI, N. et al. Effect of pore size on bone ingrowth into porous titanium implants fabricated by additive manufacturing: An in vivo experiment. **Materials Science and Engineering C**, v. 59, 2016.

TEIXEIRA, B. N. et al. Evaluation of Bone Marrow Stem Cells response to PLA scaffolds manufactured by 3D printing and coated with Polydopamine and Collagen I. **Journal os Biomedical Materials Research Part B: Applied Biomaterials**, 2017.

TRIPATHI, B. P. et al. Enhanced hydrophilic and antifouling polyacrylonitrile membrane with polydopamine modified silica nanoparticles. **RSC Adv.**, v. 6, n. 6, p. 4448–4457, 2016.

TROHATOU, O.; ROUBELAKIS, M. G. Mesenchymal Stem/Stromal Cells in Regenerative Medicine: Past, Present, and Future. **Cellular Reprogramming**, v. 19, n. 0, p. cell.2016.0062, 2017.

TSAI, W. B. et al. Poly(dopamine) coating of scaffolds for articular cartilage tissue engineering. **Acta Biomaterialia**, v. 7, n. 12, p. 4187–4194, 2011.

TYLER, B. et al. Polylactic acid (PLA) controlled delivery carriers for biomedical applications. **Advanced Drug Delivery Reviews**, v. 107, p. 163–175, 2016.

VACANTI, J. P.; LANGER, R. Tissue engineering: the design and fabrication of living replacement devices for surgical reconstruction and transplantation. **Lancet**, v. 354, p. SI32-I34, 1999.

VAEZI, M.; SEITZ, H.; YANG, S. A review on 3D micro-additive manufacturing technologies. **International Journal of Advanced Manufacturing Technology**, v. 67, n. 5–8, p. 1721–1754, 2013.

VINARDELL, T. et al. Chondrogenesis and integration of mesenchymal stem cells within an in vitro cartilage defect repair model. **Annals of Biomedical Engineering**, v. 37, n. 12, p. 2556–2565, 2009.

WANG, M. O. et al. Evaluating 3D-printed biomaterials as scaffolds for vascularized bone tissue engineering. **Advanced materials (Deerfield Beach, Fla.)**, v. 27, n. 1, p. 138–144, 2015a.

WANG, T. et al. Osteoinduction and proliferation of bone-marrow stromal cells in

three-dimensional poly (ε-caprolactone)/ hydroxyapatite/collagen scaffolds. **Journal of Translational Medicine**, v. 13, n. 1, p. 152, 2015b.

WU, S. et al. Biomimetic porous scaffolds for bone tissue engineering. **Materials Science and Engineering R: Reports**, v. 80, n. 1, p. 1–36, 2014.

XIONG, G. et al. Enhanced biological behavior of bacterial cellulose scaffold by creation of macropores and surface immobilization of collagen. **Macromolecular Research**, v. 23, n. 8, p. 734–740, 2015.

YANG, J.; BEI, J.; WANG, S. Enhanced cell affinity of poly (D,L-lactide) by combining plasma treatment with collagen anchorage. **Biomaterials**, v. 23, n. 12, p. 2607–2614, 2002.

YEH, C. H. et al. Poly(Dopamine)-assisted immobilization of Xu Duan on 3D printed poly(Lactic Acid) scaffolds to up-regulate osteogenic and angiogenic markers of bone marrow stem cells. **Materials**, v. 8, n. 7, p. 4299–4315, 2015.

YU, B. et al. Enhance the Bioactivity and Osseointegration of the Polyethylene-Terephthalate-Based Artificial Ligament via Poly(Dopamine) Coating with Mesoporous Bioactive Glass. **Advanced Engineering Materials**, v. 19, n. 5, p. 1600708, maio 2017.

YU, X.; WALSH, J.; WEI, M. Covalent immobilization of collagen on titanium through polydopamine coating to improve cellular performances of MC3T3-E1 cells. **RSC Advances**, v. 4, n. 14, p. 7185, 2014.

ZHANG, Q. et al. Pore size effect of collagen scaffolds on cartilage regeneration. **Acta Biomaterialia**, v. 10, n. 5, p. 2005–2013, 2014.

ZIEMIAN, C. W.; CRAWN, P. M. Computer aided decision support for fused deposition modeling. **Rapid Prototyping Journal**, v. 7, n. 3, p. 138–147, 2001.

Appendix 1 - Publications

Peer-reviewed publications

- B. N. TEIXEIRA, P. APRILE, R. H. MENDONÇA. D. J. KELLY e R. M. S. M THIRÉ. " Evaluation of Bone Marrow Stem Cells Response to PLA Scaffolds Manufactured by 3D printing and coated with Polydopamine and Type I Collagen" Journal of Biomedical Materials Research: Part B - Applied Biomaterials (2017) - http//onlinelibrary.wiley.com/journal/10.1002/(ISSN)1552-4981 Impact Factor: 3.189/ Qualis A1 em Engenharias II - Provisional acceptance
- B.N. TEIXEIRA, M.O.C. MAIA-PINTO, D.J. KELLY, R.M.S.M. THIRÉ. "Effect of Pore Size on Properties of 3D Printed Poly(lactic acid) Scaffolds Applied to Bone Tissue Engineering" submitted to Advances in Materials Science and Engineering (2017) - https://www.hindawi.com/journals/amse/. Impact Factor: 1.299/ Qualis A2 em Engenharias II - Submitted

Conference Papers

- TEIXEIRA, B. N.; MAIA-PINTO, M.O.C.; CALAZANS-MAIA, M.D.; KELLY, D. J. ; THIRÉ, R.M.S.M. Structural evaluation of pla scaffolds obtained by 3d printing via fused deposition modeling (fdm) technique for applications in tissue engineering. In: 5° OBI, Maresias, São Paulo. Anais do 5° OBI, 2017
- TEIXEIRA, B. N.; KELLY, D. J.; THIRÉ, R.M.S.M. . Evaluation of BMSCs response to PLA Scaffolds produced by FDM and Coating with Dopamine and 88 Collagen. In: 9º COLAOB - Congresso Latino Americano de Órgãos Artificiais, Biomateriais e Engenharia de Tecidos, 2016, Foz do Iguaçú. Anais do 9º COLAOB, 2016.
- CARDOSO, P. H. M. ; TEIXEIRA, B. N. ; VASCONCELOS, L. C. ; OLIVEIRA, M. G. ; BASTIAN, F.L. ; THIRÉ, R.M.S.M. . Efeito de parâmetros de processamento nas propriedades mecânicas e na morfologia de peças

produzidas por impressão 3D. In: 13º Congresso Brasileiro de Polímeros - CBPol, 2015, Natal. Anais do 13º Congresso Brasileiro de Polímeros, 2015

Abstract in conferences:

- TEIXEIRA, B. N.; APRILE, P.; THIRÉ, R.M.S.M.; KELLY, D. J. . Stem cell response to 3D printed PLA scaffolds functionalised with polydopamine and collagen. In: 22nd Bioengineering in Ireland - BINI, 2016, Galway. Book of Abstract. Galway: NUI Galway, 2016. p. 79.